TKK Dissertations 99
Espoo 2007

RATE EQUATION MODELING OF HYPERTHERMAL SURFACE GROWTH

Doctoral Dissertation

Mika Olavi Jahma

Helsinki University of Technology
Department of Engineering Physics and Mathematics
Laboratory of Physics

TKK Dissertations 99
Espoo 2007

RATE EQUATION MODELING OF HYPERTHERMAL SURFACE GROWTH

Doctoral Dissertation

Mika Olavi Jahma

Dissertation for the degree of Doctor of Science in Technology to be presented with due permission of the Department of Engineering Physics and Mathematics for public examination and debate in Auditorium F at Helsinki University of Technology (Espoo, Finland) on the 14th of December, 2007, at 12 noon.

Helsinki University of Technology
Department of Engineering Physics and Mathematics
Laboratory of Physics

Teknillinen korkeakoulu
Teknillisen fysiikan ja matematiikan osasto
Fysiikan laboratorio

Distribution:
Helsinki University of Technology
Department of Engineering Physics and Mathematics
Laboratory of Physics
P.O. Box 1100
FI - 02015 TKK
FINLAND
URL: http://www.fyslab.tkk.fi/
Tel. +358-9-451 3101
Fax +358-9-451 3116
E-mail: fyslab@hut.fi

© 2007 Mika Olavi Jahma

ISBN 978-951-22-9113-7
ISBN 978-951-22-9114-4 (PDF)
ISSN 1795-2239
ISSN 1795-4584 (PDF)
URL: http://lib.tkk.fi/Diss/2007/isbn9789512291144/

TKK-DISS-2393

Picaset Oy
Helsinki 2007

HELSINKI UNIVERSITY OF TECHNOLOGY P. O. BOX 1000, FI-02015 TKK http://www.tkk.fi	ABSTRACT OF DOCTORAL DISSERTATION

Author Mika Jahma

Name of the dissertation
Rate Equation Modeling of Hyperthermal Surface Growth

Date of manuscript 15. 10. 2007	Date of the dissertation 14. 12. 2007
☐ Monograph	☒ Article dissertation (summary + original articles)

Department	Department of Engineering Physics and Mathematics
Laboratory	Laboratory of Physics
Field of research	Computational Physics
Opponent(s)	Professor Karsten Albe
Supervisor	Professor Tapio Ala-Nissilä
(Instructor)	Docent Ismo T. Koponen

Abstract

The miniaturization of electronics in the past decades has lead to a situation where the size of current state-of-the-art microelectronic devices is approaching the nanometer length scale. The current methods of microelectronics, which can be used to control the fabrication of the manufacturing on atomic level, can be used only in limited conditions, and new methods are needed. This is especially acute as the recent advances in *nanotechnology* have given new tools for further development in microelectronics. Molecular Beam Epitaxy (MBE) is currently perhaps the most important atomic scale method for fabricating epitaxial thin films. The quality of films is very high and control over the growth of them is possible on the atomic scale. However, the MBE method works only under quite restricted growth conditions. At low temperatures it often leads to rough surfaces and three dimensional structures instead of smooth epitaxial films. The same happens when the deposition flux is increased. The limiting factor is the rate of surface diffusion, which should be high compared to the deposition rate, in which case the deposited atoms have enough time to diffuse on the surface and form clusters.

In this Thesis submonolayer growth has been studied using Rate Equation formulation. Rate equations provide a flexible and computationally effective tool to model complex island growth phenomena and are particularly suitable in ion beam assisted deposition (IBAD) and low energy ion deposition (LEID) type of growth conditions. In IBAD and LEID the surface is under constant ion bombardment and growth is thus explicitly a nonequilibrium phenomenon. The advantage of such Hyperthermal Deposition (HTD) methods over the MBE is a higher deposition rate during the growth process. Also, control over the quality of the atomic layers is better.

The results presented in this Thesis suggest that there is possible improvement to be gained from experimental studies of submonolayer island growth. A more detailed knowledge of diffusion of islands on different surfaces and the detailed measurements of island break-up probabilities under various growth conditions could lead to more quantitative descriptions of growth in computationally inexpensive and flexible models, which could be used to find the optimal growth conditions and extend the limits of the current thin film manufacturing methods.

Keywords Island growth, IBAD, LEID, Rate Equations, Particle Coalescence Method

ISBN (printed) 978-951-22-9113-7	ISSN (printed) 1795-2239
ISBN (pdf) 978-951-22-9114-4	ISSN (pdf) 1795-4584
ISBN (others)	Number of pages 92 p. + app. 52 p.

Publisher Laboratory of Physics, Helsinki University of Technology

Print distribution Laboratory of Physics, Helsinki University of Technology

☒ The dissertation can be read at http://lib.tkk.fi/Diss/2007/isbn9789512291144/

VÄITÖSKIRJAN TIIVISTELMÄ	TEKNILLINEN KORKEAKOULU PL 1000, 02015 TKK http://www.tkk.fi

Tekijä Mika Jahma

Väitöskirjan nimi

Rate Equation Modeling of Hyperthermal Surface Growth

Käsikirjoituksen päivämäärä 15. 10. 2007	Korjatun käsikirjoituksen päivämäärä 23. 11. 2007

Väitöstilaisuuden ajankohta 14. 12. 2007

☐ Monografia	☒ Yhdistelmäväitöskirja (yhteenveto + erillisartikkelit)

Osasto	Teknillisen fysiikan ja matematiikan osasto
Laboratorio	Fysiikan laboratorio
Tutkimusala	Laskennallinen fysiikka
Vastaväittäjä(t)	Professori Karsten Albe
Työn valvoja	Professori Tapio Ala-Nissilä
Työn ohjaaja	Dosentti Ismo T. Koponen

Tiivistelmä

Elektroniikan jatkuva miniatyrisointi viime vuosikymmeninä on johtanut siihen, että nykyisten mikroelektroniikan komponenttien koko lähestyy nanometrien luokkaa. Nykyiset metodit, joita voidaan käyttää myös atomaarisessa kokoluokassa elektroniikan valmistuksessa, eivät enää riitä ja niitä voidaan käyttää vain rajoittuneissa olosuhteissa, mikä on johtanut uusien menetelmien kehitystarpeeseen. Tarve on erityisen akuutti, koska *nanoteknologia* on luonut uusia konsepteja ja työkaluja mikroelektroniikan jatkokehittämiseen. Molekyylisuihkuepitaksia (Molecular Beam Epitaxy, MBE) on nykyään ehkä tärkein atomiskaalan metodi epitaktisten ohutkalvojen valmistuksessa. Saavutettu ohutkalvojen laatu on erittäin korkea ja kasvatuksen kontrollointi on mahdollista atomaarisella skaalalla. Siitä huolimatta MBE:n kasvatusolosuhteet ovat suhteellisen rajatut. Matalissa lämpötiloissa MBE johtaa usein karkeisiin pintoihin ja kolmiulotteisten rakenteiden syntyyn sen sijaan, että lopputuloksena olisi tasaisia epitaktisia atomikerroksia. Samaan tulokseen johtaa myös depositiovirran kasvattaminen

Tässä väitöskirjassa on tutkittu alhaisella peitolla saarekekasvua pinnalla käyttäen reaktionopeusyhtälömenetelmiä (Rate Equation, RE). RE:t mahdollistavat joustavan ja laskennallisesti tehokkaan tavan mallintaa monimutkaisia saarekekasvun ilmiöitä, ja ovat erityisen käyttökelpoisia ionisuihkuavusteisen deposition (Ion Beam Assisted Deposition, IBAD) ja alhaisen energian ionideposition (Low Energy Ion Deposition, LEID) tyyppisissä kasvuolosuhteissa. Näissä menetelmissä pinta on ionisuihkun aiheuttaman pommituksen alainen ja tapahtuva kasvu on puhtaasti epätasapainoilmiö. Tämänkaltaisten hypertermisten depositiomenetelmien (Hyperthermal Deposition, HTD) etu MBE:hen nähden on korkeampi depositiovuo kasvun aikana. Myöskin saavutettu laadun kontrolli on parempi

Tässä väitöskirjassa esitetyt tulokset viittaavat mahdollisuuteen kehittää entistä parempia malleja saarekekasvun kokeellisen tutkimuksen kautta. Entistä yksityiskohtaisempi saarekediffuusion tuntemus erilaisilla pinnoilla ja yksityiskohtaiset kokeet saarekkeiden hajoamisprosesseista erilaisissa kasvuolosuhteissa johtaisivat parempaan kvantitatiiviseen kasvun kuvaukseen käyttäen laskennallisesti kevyitä ja joustavia malleja, joiden avulla optimaalisten kasvuolosuhteiden löytäminen ja nykyisten ohutkalvojen valmistusmenetelmien käyttöalueen laajentaminen olisi mahdollista.

Asiasanat Saarekekasvu, ohutkalvot, ioniavusteinen depositio, hyperterminen depositio, reaktionopeusyhtälöt

ISBN (painettu) 978-951-22-9113-7	ISSN (painettu) 1795-2239
ISBN (pdf) 978-951-22-9114-4	ISSN (pdf) 1795-4584
Kieli Englanti	Sivumäärä 92 s. + liit. 52 s.

Julkaisija Fysiikan laboratorio, Teknillinen korkeakoulu

Painetun väitöskirjan jakelu Fysiikan laboratorio, Teknillinen korkeakoulu

☒ Luettavissa verkossa osoitteessa http://lib.tkk.fi/Diss/2007/isbn9789512291144/

Preface

This Thesis was started in Department of Physical Sciences at University of Helsinki, under supervision of Dr. Ismo T. Koponen, and was completed in the group of Prof. Tapio Ala-Nissilä, a part of Computational Nanoscience (COMP) group, an Academy of Finland Center of Excellence, at Helsinki University of Technology. I would like to thank Dr. Marko Rusanen for providing me the theoretical background of Rate Equations and many indispensable discussions around the coffee table in the small coffee room of Physics Laboratory — thank you for all the professional discussions and guidance in these years. I also thank Prof. Kai Nordlund, Dr. Jonas Frantz and Prof. Talat S. Rahman for great collaborations which lead to publications.

The social circles of the Physics Laboratory are large and I cannot possibly mention all the people in this short note. However, there are some people I must thank personally. My colleagues at that time Sami Majaniemi, Esa Kuusela, Sampsa Jaatinen, Emma Falck and Emma Terämä — it was reassuring to see you complete your doctoral studies, and it gave me the inspiration to do it also. Also Emppu Salonen, Jari Jalkanen and Kirsi Riekki provided good travel company abroad. I thank Mikko Heikkilä at Laboratory of Inorganic Chemistry, Department of Chemistry of Helsinki University for useful comments. Finally, I thank all the people I did not mention by name but had good time with during my time in the Laboratory of Physics, I think you know who you are.

The financial support from the Väisälä Foundation, the Finnish Cultural Foundation and the National Graduate School in Materials Physics is gratefully acknowledged.

Espoo, October 2007

Mika Jahma

Contents

Preface **7**

Contents **9**

List of Publications **11**

Author's contribution **13**

List of Abbreviations **15**

List of Symbols **17**

1 Introduction **19**

2 Surface growth and basic atomistic processes in hyperthermal deposition **25**

2.1 Experimental methods of controlled atomistic growth 25

2.2 Ion beam assisted deposition 28

2.3 Low energy ion deposition 29

2.4 Phenomenology of ion beam assisted surface growth 30

2.4.1 Effects of deposition in submonolayer regime 30

2.4.2 Diffusion and aggregation of islands 31

2.4.3 Island break-up and detachment 33

2.4.4 Vacancy creation and erosion 34

2.4.5 Interlayer processes 35

3 Modeling submonolayer growth and erosion **37**

3.1 Rate equations in growth 37

3.2 Rate equation for aggregation-detachment 39

3.2.1 Deposition 40

3.2.2 Diffusion and aggregation 40

3.2.3 Island break-up 43
3.3 Rate equations for aggregation-detachment-recombination of islands and vacancies 44
3.4 Scaling in rate equations 49
3.5 Method for solving the rate equations 50
3.6 Results 52
3.6.1 Transition in the growth exponent of IBAD 52
3.6.2 Anomalously high adatom density in LEID 53
3.6.3 Detachment modeled using Molecular Dynamics 55
3.6.4 Realistic diffusion rates for copper surfaces 55
3.6.5 Properties of growth in IBAD with vacancy creation 59
3.7 Conclusions on submonolayer growth 65

4 From Submonolayer to Multilayer growth **69**

5 Summary and discussion **79**

Bibliography **83**

List of Publications

This thesis consists of an overview and of the following publications which are referred to in the text by their Roman numerals.

I I. T. Koponen, M. O. Jahma, M. Rusanen, and T. Ala-Nissila, "*Submonolayer Growth with Anomalously High Island Density in Hyperthermal Deposition*", Physical Review Letters **92**, 086103, (2004). 4 pages.

II J. Frantz, M. O. Jahma, K. Nordlund, and I. T. Koponen, "*Low-energy deposition of Co onto Co islands on Ag(100): Effect on submonolayer growth*", Physical Review B **71**, 075411 (2005). 8 pages.

III M. O. Jahma, I. T. Koponen and M. Rusanen, "*Island size distributions in submonolayer growth in hyperthermal deposition*", Surface Science, Volumes **566–568**, Part 1, Proceedings of the 22nd European Conference on Surface Science, 20 September 2004, Pages 170–174.

IV M.O. Jahma, M. Rusanen, A. Karim, I.T. Koponen, T. Ala-Nissila and T.S. Rahman, "*Diffusion and submonolayer island growth during hyperthermal deposition on Cu(1 0 0) and Cu(1 1 1)*", Surface Science, Volume **598**, Issues 1–3, 20 December 2005, Pages 246–252.

V M. O. Jahma, I.T. Koponen and T. Ala-Nissila, "*Optimal conditions for submonolayer nanoisland growth in ion beam assisted deposition* ", Surface Science, Volume **601** 5628–5634 (2007). In press (Surface Science). doi:10.1016/j.susc.2007.09.037

VI T. Huhtamäki, M.O. Jahma and I.T. Koponen, "*A simple model for quantifying the degree of layer-by-layer growth in low energy ion deposition of thin films*", Nuclear Instruments and Methods in Physics Research Section B **264** 55–60 (2007), doi:10.1016/j.nimb.2007.08.073.

Author's contribution

The author Mika Jahma has had an active role in all phases of the research reported in this Thesis. The author has had the main responsibility of the calculation and the scientific analysis of the results presented in the publications. The author has taken part in writing and editing of all the presented publications.

The author has developed major parts of computer code needed in calculation and analysis of the results. The author provided the results presented in **Paper I**. The author provided the results and analysis of the Rate Equation modeling part in **Paper II**, which was a result of collaborative work with Professor Kai Nordlund and his student Jonas Frantz, who provided the results and analysis of Molecular Dynamics simulations. The author has provided all the results of Rate Equation calculations in **Paper III** and **Paper IV**. The author has written the computer program for the calculation in **Paper V** and written the draft and provided the results in that publication. The author has made essential contributions in writing the **Paper VI**, for which the calculations were provided by T. Huhtamäki and the draft was written by Ismo T. Koponen.

List of Abbreviations

ALD Atomic Layer Deposition

CVD Chemical Vapor Deposition

DFT Density Functional Theory

IBAD Ion Beam Assisted Deposition

HTD Hyper Thermal Deposition

KMC Kinetic Monte Carlo

KRE Kinetic Rate Equation

LEED Low Energy Electron Diffraction

LEID Low Energy Ion Deposition

MBE Molecular Beam Epitaxy

MD Molecular Dynamics

PCM Particle Coalescence Method

STM Scanning Tunneling Microscope

TEAS Thermal Energy Helium Atom Scattering

RE Rate Equation

RHEED Reflection High Energy Electron Diffraction

UHV Ultra High Vacuum

List of Symbols

$\bar{s}$ The mean island size

n_s The island density of islands of size s

θ Coverage of the deposited particles on the surface. Full monolayer corresponds to $\theta = 1$

Φ Deposition flux in terms of monolayers per second

M_k k^{th} moment of a distribution; i.e. $M_k = \sum_{s=1}^{\infty} s^k n_s$

δ_{ij} Kronecker δ-symbol. $\delta_{ij} = 0$ if $i \neq j$, and $\delta_{ij} = 1$ if $i = j$

β Growth exponent (see 3.4 for details)

δ Scaling exponent (see 3.4 for details)

K_{ij} Aggregation kernel

F_{ij} Fragmentation kernel. Relates to the fragmentation rate simply by $F_{ij} = F_{i+j}$

1 Introduction

The miniaturization of electronics in the past decades has lead to a situation where the size of current state-of-the-art microelectronic devices is approaching the nanometer length scale. This means new challenges in manufacturing of electronics, as the current methods have already attained the accuracy limit on the physical basis. The current methods of microelectronics, which can be used to control the manufacturing on atomic level, can be used only in limited conditions, and new methods are needed. This is especially acute as the recent advances in nanotechnology have given new tools for further development in microelectronics. New *nanoelectronic* devices have surfaced and have proved to provide effective solutions, if the corresponding manufacturing methods can be scaled up into industrial use.

On the nanoscale novel phenomena and structures emerge, because the nanoscale approaches the typical length scale of basic atomic phenomena. The fabrication of *nanodots* and *nanopatterns* involves knowledge of the basic properties of the constituents from which these objects are created. Furthermore, *thin films* of single atomic layer thickness are constituents of new functional materials for nanotechnology [1].

Molecular Beam Epitaxy (MBE) is currently perhaps the most important atomic scale method for fabricating epitaxial thin films. The quality of films is very high and control over the growth of them is possible on the atomic scale (the lateral dimension of structures on surface is below 100 nanometers; thickness of a single epitaxial film layer is of order of single atomic spacing in a bulk crystal). In MBE atoms are deposited on the surface from a gas phase in high vacuum conditions, and they are let to diffuse on the surface. Diffusion leads to nucleation of small islands if the surface is kept in favorable conditions so that islands eventually coalesce in late stages of the layer completion and form epitaxial films. Continued deposition of

new atoms leads eventually to the formation of multiple atomic layers of deposited material.

However, the MBE method works only under quite restricted growth conditions. At low temperatures it leads often to rough surfaces and three dimensional structures instead of smooth epitaxial films. The same happens when the deposition flux is increased. The limiting factor is the rate of surface diffusion, which should be high compared to the deposition rate, in which case the deposited atoms have enough time to diffuse on the surface and form clusters. In the case where diffusion is weak the deposition will randomly occur on immobile clusters and stay there. This leads to roughening of the surface.

More control over the growth may be attained by using Hyperthermal Deposition (HTD), which uses an external accelerated ion source to bombard the surface during growth. This is called the Ion Beam Assisted Deposition (IBAD) method. In IBAD it is possible to suppress many growth instabilities which would lead to mounding and roughening of the surface. Ion bombardment with a controlled impact energy of 10 eV to 1 keV is used to break up any emerged large structures on the surface, and as a result the nucleated islands will stay relatively small, with sizes up to few tens of atoms. This will suppress the growth of large islands already in the initial stage of growth, hinder their coalescence to even larger islands, and keep the islands small enough throughout the growth until the layer is nearly completed, so that second layer nucleation is suppressed up to the stage of layer completion. The same effect can be attained in Low Energy Ion Deposition (LEID) where the deposition flux itself is accelerated and causes single atoms to detach from large islands. Additionally, the bombardment will cause enhanced mobility of the surface adatoms, which will still accelerate the aggregation of adatoms into islands and promote small island nucleation. Furthermore, bombardment will cause surface vacancies to be created on the substrate layer. The vacancies will act as sites for excess adatoms to fall in. This will further regulate growth as shown in Paper V.

Conventional simulation methods such as Molecular Dynamics are inadequate in modeling growth phenomena due to the large amount of single atom diffusion processes present on surface under hyperthermal growth conditions. In general, modeling surface growth is very complicated and simulation studies must be simplified greatly due to the vast difference in the time scales of the different phenomena. For example, monomer diffusion on surfaces is several orders of magnitude faster than any significant growth phenomena. In hyperthermal growth the aggregation rate to deposition rate ratio is of order 10^5 (Paper I), i.e. there are one hundred thousand aggregation events for one deposition event. Thus simulation study must cover large differences in time scales, and this makes the simulation very demanding computationally, unless great simplifications are made. In determining size distributions this rules out any first principles methods, as well as classical Molecular Dynamics, due to their limited simulation time span.

Modeling of the deposition conditions using realistic surface aggregation rates is possible in a very simple yet effective framework based on reaction kinetic description of the system. The reaction kinetic description originates from the work done by Marian Smoluchowski. He proposed a Rate Equation formulation to model coagulation in solutions in 1916 [2, 3]. Since then the rate equations have been used in a wide variety of applications, ranging from material science [4] to biology [5], and even in financial analysis [6] and astrophysics [7]. The rate equation approach has been chosen in the present Thesis for its ability to provide insight in the growth problem, which is complex by nature. The rich phenomenology of surface structure formation calls for methods with which various effects can be separated and controlled individually. On phenomenological level rate equations provide a flexible tool to construct models for complex non equilibrium kinetic problems.

First and foremost, it is necessary to understand first layer growth. All subsequent structure formation is bound to begin from submonolayer growth. The knowledge of effects on growth in the submonolayer regime will translate to greater understand-

ing of growth of complex structures on surfaces. Surface growth has been studied in the last decade intensively since the surface imaging techniques improved dramatically when the scanning tunneling microscope was developed in the early 80's. The abundance of measured data of growing surfaces has increased the need for semimicroscopic modeling.

The need for simulating large time scales and large systems calls for efficient models and effective coarse-graining. It is not possible to treat individual atoms in large scale models. In rate equation modeling the basic unit is a point-like island on the surface, and all the explicit atomistic processes are treated on an average level. In submonolayer growth the most important phenomenon is the diffusion of adatoms on the surface, which is the driving force for island growth. From the point of view of rate equation models, diffusion enters in the form of aggregation rate function. In solving the rate equations the effect of diffusion comes in only trough the effective reaction rates, but otherwise the reaction kinetic (RK) description ignores spatial correlations. Technically, this kind of model is often referred to as the mean field level description. Using the RK scheme based on mean field description gives access to larger time scales in computation, and also to larger ensembles, and allows to explore the size-configuration space more thoroughly (to obtain size distributions) than the Kinetic Monte Carlo (KMC) or Molecular Dynamics (MD) schemes.

It is possible to incorporate some of the geometric information about the surface into the rate equations through the aggregation rate function. Diffusion on different surfaces is distinctly different and the form of the aggregation rate function will reflect the nature of diffusion on the average level. To explore the effects of diffusion on growth we have used realistic diffusion coefficients of Cu(1 0 0) and Cu(1 1 1), as well as Pt(1 1 1), in rate equations. The calculations show that on the qualitative level the growth follows the same trends, even though the quantitative results change to reflect the different physical system under inspection. We show that in IBAD conditions the growth is robust and the minute details of the basic atomic processes

are averaged out from the end results. This also explains why the IBAD picture is applicable in quite wide a regime of growth conditions.

The aim of this Thesis is to study effects of microscopic diffusion, aggregation and detachment processes on the submonolayer growth of islands and in particular how they are reflected on the properties of island size distributions under the conditions of HTD. The focus is on the properties which might be experimentally accessible in current HTD experiments. To this end we have studied the rate equation model for the *aggregation-detachment* picture for submonolayer growth (See Paper I). The assumed mode of detachment in Paper I was then confirmed by Molecular Dynamics simulations in Paper II. In Paper III we compared the IBAD and LEID methods from the point of view of rate equation modeling and retrieved the island size distribution functions and growth exponents for both cases. It was also suggested that the island break-up process is different in these cases. In Paper IV we used realistic islands diffusion on Cu(1 0 0) and Cu(1 1 1) in rate equations and showed that the general properties of growth are robust in the sense that small changes in rate coefficients are not enough to completely change the growth mode. In Paper V we introduce the rate equation model for island growth where vacancies form on the substrate layer. In this model the adatoms are allowed to drop into the vacancies as well as to aggregate into islands. The interlayer processes introduced have a profound effect on the growth and are shown to promote layer-by-layer growth. In Paper VI we introduce a simple model for multilayer growth based on interlayer mass transport.

The Thesis has been divided into four parts. The basic phenomena on a surface undergoing submonolayer island growth are reviewed in Section 2. The formulation of rate equations for growth is presented in Section 3 and in Section 3.6 the main results are given. The transition into slow layer-by-layer growth found in Paper I is explained and summarized. The effects of differences in diffusion on Cu(1 0 0) and Cu(1 1 1) on the island size distributions and effective scaling are analyzed. Also, the growth situation where vacancies on the surface are allowed is shown to be

able to further regulate growth and promote layer-by-layer growth. In Section 4 we take a look into multilayer growth and address the effects of basic kinetic processes of submonolayer regime when approaching optimal multilayer growth. In the last Section 5 the progress achieved in the Thesis is summarized.

The questions that remain unresolved are the role of coalescence in layer filling in the late stage of first layer growth, the details of second layer nucleation, and whether it is possible to create simplified description of the processes involved to be combined to the existing rate equation models. The emphasis in this Thesis is on the phenomenological level of description of growth proceeding from submonolayer regime to controlled multilayer growth. To this end further progress can be achieved by combining experimental studies and the rate equation approach to bring detailed information on the growth conditions on the atomic level into phenomenological model.

2 Surface growth and basic atomistic processes in hyperthermal deposition

2.1 Experimental methods of controlled atomistic growth

Perfect epitaxy in materials grown from an external source of atoms or molecules can be achieved by multitude of methods. Molecular Beam Epitaxy (MBE) [8], Chemical Vapor Deposition (CVD) [9] and Atomic Layer Deposition (ALD) [10] are methods which have been known for over a quarter of a century. All these methods utilize atomistic or molecular forms of material as the starting point for assembly of layers, structures or patterns on the surfaces. In these methods thin films, which are several atomic layers thick, are produced in great accuracy. However, it still remains a challenge to extend the conditions, which can be used to produce single atomic layers one by one, to create perfect ordered overlayers.

Even though MBE is capable of producing single crystal overlayers, the associated growth rate is often impractical if industrial scale of production is desired, and there is need to improve the growth rate and the conditions where high growth rates can be sustained without compromising the quality of the produced atomic films. Thus accelerated single crystal growth methods are needed. A standard way of implementing MBE on surfaces is by using a heated source that emits atoms from its own surface, and then letting the heated atoms to travel on the substrate located in the vicinity of the source. The deposition energies will be *thermally distributed* and directly related to the evaporation temperature. Control over the deposition energy and flux is limited in this method.

There exists several deposition methods using accelerated source of atoms, which differ in their typical particle energy, and may include additional ion bombardment

or use a special deposition potential between the particle source and the substrate to control the deposition energy with greater accuracy.

Hyperthermal deposition (HTD) techniques have recently become an important tool in improving and controlling the properties and growth of thin films during deposition. They include low-energy ion deposition (LEID) [11] and ion beam assisted deposition (IBAD) [12] techniques. Under optimal conditions thin films with improved smoothness can be obtained under much less stringent deposition conditions than in ordinary molecular beam epitaxy (MBE) [12–14].

In methods based on HTD it is typical that the surface is under an external particle flux. Incoming particles carry energy in their motion and release it completely or partially when they hit the surface. Depending on the structure of the surface and the incoming particles various dissipative processes will then spread the kinetic energy of the particle on the surface and usually modify the surface structure somehow, and also heat up the surface initiating other processes on the surface, i.e. diffusion of small islands on the surface (See Figure 2.1 for a schematic picture of the surface growth conditions). This is in contrast to thermal deposition methods, in which the adsorbed atoms carry a minimal extra energy to be able to be stuck to the surface, and thus in thermal deposition methods the surface growth cannot be controlled externally.

In HTD it has been observed that island growth can be very different from ordinary thermal deposition. Typical improvements are that the island density is larger, the average island size is smaller [12–14], and island size distributions are much broader [11, 12], when compared to those created by thermal deposition. Various atomistic processes such as ion enhanced mobilities, cluster dissociation [11], and defect creation [13–15] have been suggested to explain this. Enhanced nucleation of small islands due to displaced surface atoms is shown to have a decisive role in growth on fcc(111) surfaces [13, 14, 16] but similar effects on growth have been

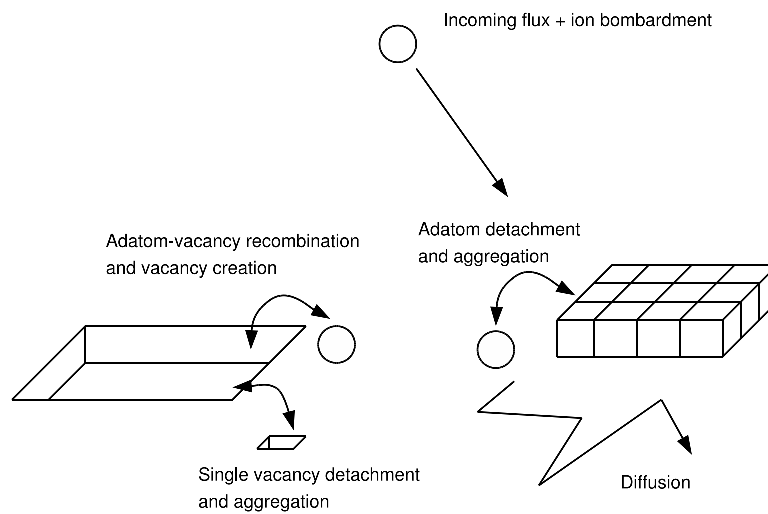

Figure 2.1: Typical atomistic processes on a growing surface are shown schematically. Incoming flux of adatoms either sticks on the surface or lands on an already formed island and induces adatom detachment. External ion bombardment can also cause island break-up. On the substrate surface bombardment causes vacancy creation which through surface vacancy diffusion leads to vacancy island nucleation. Adatoms may be incorporated either into islands or vacancies, which is true for single vacancies also.

demonstrated to be caused by fragmentation and detachment, too [11].

2.2 Ion beam assisted deposition

Ion beam assisted deposition (IBAD) of thin films is a technique where energetic ion beams with energies ranging from a few tens of eV up to a few keV are used to enhance smooth epitaxial growth. The ratio of bombarding ions to the deposited atoms is kept moderately low, and can range from 0.1% to 10% [12–14, 17, 18]. In IBAD the impacts of the energetic ions prevent the onset of three-dimensional (3D) growth mode and the surface can be kept in two-dimensional (2D) layer-by-layer growth mode. This leads to layers with improved smoothness [19, 20].

In IBAD the impact energies are large enough to cause displacement and sputtering of the surface atoms, and in the case of metallic films impacts energies larger than 50 eV have a substantial probability to displace an adatom thus effectively creating a vacancy-adatom pair [19, 20]. The redistribution of surface atoms caused by impacts of the energetic ions helps to increase the nucleation of new islands [12–14], due to the increased adatom concentration. In addition, ion bombardment also facilitates interlayer mass transport processes [15, 19, 20]. These conditions can be created with IBAD just by increasing the energy and number of impacts.

If the ion bombardment energy is still increased creation of vacancies on the substrate starts. When the vacancy creation rate is large enough, the vacancies begin to aggregate and vacancy islands start to grow. If the bombardment energy is increased further, the surface may begin to erode and roughen, in which case the benefits of IBAD are lost. At high bombarding energies above 1 keV surface growth may still occur, because vacancy clusters are created beneath the surface, and ion bombardment causes adatom island formation due to the sputtered atoms on the surface [21]. However, at low bombarding energies well below 1 keV, where approximately one

vacancy defect per impact is created, the vacancy defects remain on the surface and only one adatom on the surface is produced. The surface vacancy defects will be mostly annealed out, but vacancy clusters may still remain on the surface [19, 21].

In this work, we develop a rate equation model for IBAD. In the model the reaction kinetic rates serve as the primary parameters instead of the ion energy and mass [22, 23]. It remains an independent task to relate the kinetic reaction rates to the parameters describing the bombardment in various special cases. The kinetic reaction rates can be acquired either through simulations or analytically (see e.g. refs. [23, 24] and references therein).

2.3 Low energy ion deposition

Low energy ion deposition is a technique where accelerated ions have a well controlled *soft landing potential* between the source and the substrate. The ions are slowed down to a desired deposition energy very accurately. Additional ion bombardment is not used. In LEID it's a remarkable fact that the properties of growth and the associated size distributions do not seem to depend much on the details of ion bombardment. With different deposition energies an anomalously high density of small islands is observed with very similar distributions [11].

This is unexpected, since microscopic surface processes such as target adatom creation, additional kink site creation and "chipping" off of adatoms from island edges do depend sensitively on the details of bombardment [15, 20]. In LEID the number of additional detachment events due to deposition is relatively low, and thus it is not obvious how an anomalously high island density is maintained. The basic processes and phenomena on the growing surface are reviewed below. Detailed knowledge of these processes is crucial in the development of more simplified and flexible models to be used to obtain island size distributions, and to study island growth and surface

roughening during growth.

2.4 Phenomenology of ion beam assisted surface growth

2.4.1 Effects of deposition in submonolayer regime

The way an incoming flux modifies the surface is strongly dependent of the kinetic energy of the particles in the flux. Moderately energetic ions of energies 1 keV and up will penetrate the surface and generate a substrate vacancy below the surface. The elevated substrate atoms will emerge on the surface and some of them will sputter away. Clearly this is detrimental to the surface quality and will prevent any layer-by-layer growth.

By lowering the incident energy of the ions sufficiently one can find an optimal value for the incident energy brought to the surface by ions (see Paper V for details), for which the ion bombardment ceases to create too many vacancies. At this stage the effect of ion bombardment is to create just enough vacancies to keep interlayer processes active, and also to break up large islands. These processes will help keeping the surface growth in layer-by-layer mode through preventing second layer nucleation from starting. Section 2.4.5 discusses this in detail.

Low energy ion deposition provides external control over deposition [25] by using an additional potential between the ion source and the substrate. This makes it possible to specify the deposition energy very accurately. In LEID external ion bombardment is not used. However, incoming deposition flux will hit also large islands on the surface and transfer energy to them. This will cause an additional effective adatom flux on the surface due the detachment from the edge of the large islands.

2.4.2 Diffusion and aggregation of islands

Diffusion of adatoms on the surface is the most important process affecting island growth in the submonolayer regime. The deposited adatoms will diffuse in the vicinity of their adsorption site until they meet another adatom, an island, an step edge or a vacancy. The diffusion properties of the surface species, i.e. adatoms and islands, depend strongly on the structure of the surface. In this work we have mainly concentrated on the copper fcc (1 0 0) and (1 1 1) surfaces, because they are simple enough systems to be tractable from the point of view of modeling and computation, but they at the same time display the important characteristic features present in more complex situations. In particular, they exhibit notably different island diffusion coefficients (see Paper IV).

The diffusive time scales vary enormously on the surface. Compact islands are practically immobile, but they can diffuse, whereas adatoms are very mobile in temperatures in which growth can happen. A surface under particle flux is heating up due the energy transferred by irradiation, but in practice the temperature is fairly well controlled and kept at about $T \sim 200K \dots 400K$. On the copper (1 1 1) surface the fastest diffusing species is a dimer in contrast to the copper (1 0 0), where the fastest are adatoms. Compact islands are mostly immobile whereas islands with complicated geometry can exhibit concerted diffusion mechanisms, through which they may attain a finite diffusion coefficient. In this case the diffusion coefficient as function of island size exhibits distinct oscillatory behavior. These mechanisms are discussed in detail in Section 2.4.2.

The aggregation of adatoms into larger structures is driven by surface diffusion of the adatoms. Islands can diffuse, too, if the temperature of the surface is high enough to activate island diffusion processes, which usually have relatively high activation energy barriers. Islands can also diffuse through *concerted movement* processes, which can boost the diffusion rates considerably [26].

Single adatoms will diffuse on the clean surface due to thermally excited processes, which include *hopping* from a site to an other and *exchange* diffusion. On certain surfaces exchange diffusion can be more important, but in general both contribute to the diffusion rate. Thermally activated diffusion processes can be summarized in a formula, where the diffusion barrier E_D contributes to the diffusion coefficient according to the *Arrhenius law*

$$D = D_0 \exp(-E_D/kT), \tag{2.1}$$

where k is the Boltzmann constant, T is temperature and the D_0 is the diffusivity, which is dependent on the material.

Usually the are steps distributed on the surface. The steps will divide the surface into separate areas of island growth and hinder adatom diffusion trough the steps due to an additional energy barrier, called the *Ehrlich–Schwoebel barrier* on the step edge. Once caught in a step an adatom tends to diffuse preferentially along the step edge. Similarly, on a surface where some large stable islands have emerged, the diffusing adatom can be incorporated into a such an island, and can continue diffusing along the edge of the island. The edge diffusion contributes to the total *island diffusion rate.* In addition to edge diffusion islands can have other mechanisms of diffusion. Most notable is the movement of small islands due to concerted motion of atoms on the island boundary [26]. Small islands, up to size of few tens of atoms, obtain geometry which is not close to circular or compact, unless they contain certain number of atoms which enables them to have a *compact geometry.* For example on Cu(1 0 0) the four atom island clearly obtains a very stable geometry of a square. One extra atom of the pentamer has a large effect on the mobility of the island enabling several concerted modes of diffusion.

The diffusion of large islands ($\gtrsim 100$ atoms in island) can be divided into three classes [27]. *Edge diffusion* happens when the atoms in the edge of island diffuse along the edge. Large islands may also emit adatoms very rapidly, but the subsequent

diffusion of adatoms may be very slow. This leads to *terrace or surface diffusion* for the islands, where the rate limiting step is the diffusion of adatoms on the terrace. There is also *evaporation and condensation limited diffusion*, in which the rate limiting step is the evaporation and condensation at the island edge. In this mode the diffusion proceeds through evaporation of atoms from the island edge and condensation of the adatoms to it into different location on the edge, thus causing the center of mass of the island to move [28].

2.4.3 Island break-up and detachment

The incoming particle flux will at some coverage start to irradiate the islands directly. Each impact transfers energy to the island and will cause break-up processes [22] (See also Paper II). The mode of break-up depends on the impact energy. The energy scale of ion beam assisted deposition ($\sim$ 100 eV per impact) is sufficient to break an island into two or more parts (see Paper III). In low energy ion deposition the impact energy is much lower (5 eV ... 30 eV [11], see also Paper II) and only single adatoms detach from the islands. This has important effects on the growth and is clearly seen in the form of island size distribution. The implications of break-up and detachment on growth include the broadening of island size distribution and anomalously high adatom density, which are discussed in more detail in Paper II.

The most detailed information on the effect of detachment comes from experiments done by deposition of Co on Ag(001) films using LEID in recent experiments [11]. In these experiments, the morphology of the Co islands is found to be controlled by three different mechanisms: ion impact induced island fragmentation, pinning at surface-confined clusters, and ion impact induced island dissociation. It is concluded that the two first mechanisms contribute to an increased density of Co islands while the third one decreases the island density [11].

The resulting high small island density might be explained by detachment of adatoms from the edge of the islands caused by energy transfer from the ion impacts (See Paper II). This would create an additional monomer flux onto the surface, and the necessary condition for that is that the flux should be proportional to some power of the length of the island perimeter and the density of islands of that size. In contrast to this, with fragmenting islands the small island density would not increase as much, because the parts of the fragmented islands tend to be of the same order in size on the average, and the bigger the islands are, the more rare are the fragmentations of those islands. Thus, the resulting island size distribution would be very sharply peaked at the average island size. We have previously shown that the characteristic features of growth and in particular the form of island size distribution are uniquely characterized by these microscopic processes [29] (See Paper I). However, the detailed justification for the basic assumptions of the detachment model has not been given. In Paper II, we provide the necessary microscopic details to justify the crucial hypothesis put forward in our previous work (See Paper I).

2.4.4 Vacancy creation and erosion

With a sufficient incident energy surface vacancies are created. An adatom lifted from the bulk substrate onto the surface due to an impact will contribute to the adatom density. Surface vacancies will diffuse largely in the same way as adatoms and eventually form vacancy islands. Sufficiently energetic bombardment may lead to creation of large islands [21]. Large islands on the other hand may get hit by the ion bombardment on top of them, and vacancies are created there. All these mechanisms contribute to surface erosion, which then leads to a very irregular surface in the end [21] (See also Paper V). A very high incident energy will create substrate vacancies, lift atoms on the surface and sputter some of the material away. The vacancies in the substrate usually anneal out only partially, and then recombine with surface adatoms, but a significant fraction may remain to start formation of

vacancy islands and clusters, thus leading to gradual erosion.

2.4.5 Interlayer processes

Step edge or Ehrlich–Schwoebel barrier is the rate limiting energy barrier for interlayer adatom hopping. If adatoms and vacancies exist on the surface and both are allowed to diffuse on the surface, there will be a finite rate of these recombining, thus eliminating both. This recombination can have significant effects on layer-by-layer growth and the total surface smoothness.

If IBAD growth conditions are assumed, there will be an energy region in which vacancy creation is sufficient for it to control the surface growth through *interlayer recombination processes*, and keep the growing islands small, thus preventing the second layer from nucleating. The effect of recombination will depend strongly on the relative rates of the adatom flux onto surface and the vacancy creation rate, and additionally on the diffusion rates of the adatoms and vacancies. If the vacancy creation is slower than adatom deposition, which is a reasonable physical assumption in most cases, surface erosion will not take place.

The combined growth process of adatom and vacancy islands is rather complicated and a detailed description of all processes leads to model equations with a complex structure and many parameters [22, 23]. Without simplifying the description it is difficult to find any general features needed to pin down the region where IBAD is potentially applicable without causing the surface erosion or destruction instead of smooth 2D growth.

To study the effects of the reaction rates on the growth we propose a simplified description of submonolayer surface growth in cases where island and vacancy island growth takes place simultaneously. In this case vacancy creation is allowed (see

Paper V) and we find the transitional stage of growth where vacancy islands begin to be filled and eventually shrink. This borderline result gives us the limiting conditions where IBAD is still applicable without causing surface erosion or destruction. This special case needs to be examined more closely in order to clarify the exact conditions for the annealing of vacancy defects to find the optimal conditions where the bombarded surface remains smooth. In practice, this means finding the conditions where the size of the vacancy islands ultimately begins to shrink due to the effect of interlayer mass transport (adatoms filling the vacancy islands). This transition region can be detected already in the submonolayer growth region by monitoring the critical coverage where vacancy islands reach a maximum size (See Paper V for details).

3 Modeling submonolayer growth and erosion

3.1 Rate equations in growth

The current methods to model atomic phenomena differ in level of approximations made, the number of particles they are able to incorporate in the atomic model and time span they are able to simulate. The most accurate is the *ab initio* simulation method [30–32], in which single atoms and the electron density around them is calculated accurately using the density functional method. The time spans that can be reached using this method are usually of the order of a single chemical reaction, and the number of particles included in the calculation is of the order of a few hundred. However, the *ab initio* methods provide realistic force calculations between atoms and can be used to construct accurate interaction potentials for atoms.

The next step of approximation is to simulate the dynamics of atomic system using the Molecular Dynamics (MD) simulation method [33, 34], in which the positions and velocities of the atoms are included and the time evolution of the system is calculated in the classical picture. The atomic interactions may be included accurately using *ab initio* method as a basis for force calculations, or classical potential functions may be used to help the computational intensity of the problem. In MD it is possible to include tens of thousands of atoms, and the simulation time span extends to nanoseconds, while using rather realistic interatomic interactions. The system size can still be extended up to millions of atoms or the time span to microseconds if advanced calculation methods and greatly simplified interaction potentials are used for the force evaluation. The so called *hyperdynamics* method is used to accelerate the time evolution of the system by artificially activating infrequent events.

To really extend the simulation to the growth time scales Kinetic Monte Carlo

(KMC) methods [35] are used. In KMC the energy barriers of all allowed events are known *a priori*, calculated using DFT or MD or measured from a real system, and the system is reduced into a lattice where the atoms then occupy single lattice sites. Single events are then attempted and executed according to the probability of success based on the energy barriers. The *detailed balance* condition must be fulfilled so that the system is ensured to have a stable equilibrium. Even in KMC we are faced with the *time scale problem* as the single atom hopping events to the nearest neighbor sites are abundant, whereas the desired growth events take still very long simulation time spans to emerge. Also the system size is somewhat limited and only tens of islands are included in the simulation, making evaluation of the island size distribution function prone to statistical error due to limited statistical sampling.

The computational complexity can further be significantly reduced using Rate Equations (RE). Explicit atom hopping events can be summarized into an aggregation rate function. However, this approach will work only on a system in which *spatial correlations* are very weak, and regular structures that affect kinetic phenomena do not emerge. This is due to the fact that Rate Equations are an approximation of the kinetic Master Equation for the system, where the surface is isotropic and homogeneous. In this approximation all particles on the surface can mutually react with any other particle, and thus any spatial correlations are effectively averaged out of the equations. To this end the Rate Equation formulation cannot describe any structure formation. However, Rate Equations are a very effective method to acquire average growth measures, such as island size distributions and scaling exponents, if the system follows the scaling assumption (see Section 3.4) [36] (See also Paper I).

Already in 1916 Marian Smoluchowski proposed a rate equation formulation of *coagulation* [2, 3]. The *Smoluchowski equation* can be written as an infinite set of

equations coupled through the density function

$$\frac{\mathrm{d}n_s(t)}{\mathrm{d}t} = \frac{1}{2}\sum_{i+j=s} K(i,j)n_i n_j - \sum_{i=1}^{\infty} K(i,s)n_i n_s, \tag{3.1}$$

where $n_s(t)$ is the number density of the clusters of size s, and $K(i,j)$ is the coagulation kernel, which describes the physical properties of the system. The aggregation kernel denotes the total probability per unit time to aggregate two clusters with sizes i and j. In many cases of interest the kernel $K(i,j)$ is approximated to have a simple homogeneous functional form [37], so that $K(ai,aj) = a^{\lambda}K(i,j)$, where a is an arbitrary constant and λ is the *homogeneity exponent*. The aggregation probability is a function of mobility of the aggregating clusters, and is usually taken to be of multiplicative or sum form as a function of diffusion rate functions of the clusters, to make the *scaling ansatz* possible. Analytical solution for Equation 3.1 exists only in limited number of cases of $K(i,j)$ [38]. This RE scheme is limited to coagulation in cluster-cluster picture, although adatoms are included as clusters of size equal to one. This equation is used as a starting point in extension, in which break-up processes are included in the equation. The extension breaks the exact scaling scheme, but an effective scaling scheme can be used. The generalized REs do not have known exact analytical solutions, and to solve the resulting generalized REs we use a numerical approach. In the next sections this equation is extended to describe surface growth under hyperthermal deposition conditions.

3.2 Rate equation for aggregation-detachment

The rate equation model of island growth may be written in a compact form as

$$\frac{\mathrm{d}n_s(t)}{\mathrm{d}t} = f_d + f_{a,s} - f_{b,s}. \tag{3.2}$$

Here the terms on the right hand side of the equation correspond to deposition, aggregation and break-up, correspondingly. In the following the processes that con-

tribute to these terms are reviewed and a detailed description of the parameters in the terms is given.

3.2.1 Deposition

The incoming particle flux that is deposited is presented as a constant rate Φ in units of monolayers per second. The flux term in the rate equation is then

$$f_d = \Phi \delta_{1s}, \tag{3.3}$$

where the Kronecker δ-symbol restricts the incoming particle species to adatoms.

The energy transfer carried by the deposition flux to the surface must be incorporated into the aggregation and break-up rates (See Sections 3.2.2 and 3.2.3). Also, the energy transfer of additional ion bombardment is taken into account in aggregation and break-up rates.

3.2.2 Diffusion and aggregation

Island growth is driven on the surface by island diffusion. The rate to two islands to collide and form a larger island is proportional to the density of the islands and to the diffusion rate of the islands, see Eq. (3.8). We approximate this further by concluding that we may write the aggregation rate [39] as

$$K_{ij} = D_i + D_j, \tag{3.4}$$

where the logarithmic dependence on island size in the two dimensional case is omitted [40].

The specific form of D_i depends on the physical system under interest. It is common to assume that diffusion follows a power law $D_i \sim i^{-\mu}$, which makes the kernel a

homogeneous function. The homogeneity of the aggregation kernel guarantees the validity of the scaling assumption (see Sec. 3.4). On many simple metal surfaces the homogeneity exponent varies in the range $1 \leq \mu \leq 2$.

We can include some geometrical information about the surface into the model through the diffusion coefficients D_i. In Paper I we dealt with an idealized model where we set the diffusion coefficient equal to a power law as a function of island size $D_i \sim s^{-\mu}$ with $\mu = 2$, and then justified the scaling scheme in that model. This is of course a great simplification, and there is no real reason to discard the information of the details of the surface and not to use the actual diffusion coefficients of the surface at some temperature in the simulations, but we cannot obtain any analytical solutions for realistic diffusion coefficients.

We also explore in detail the influence of realistic island diffusion coefficients to submonolayer growth with HTD. To this end, we employ the RE model of Paper I and replace the usually assumed idealized power law forms of D_s with realistic, temperature and size–dependent diffusion coefficients $D_s(T)$ for Cu on Cu(1 0 0) and Cu(1 1 1) surfaces. These two systems highlight the large differences which occur for surfaces with different geometry and energetics. While the scaling function of the size distribution is largely unaffected by the details of the diffusion coefficients, the quantitative values of the growth exponents are sensitive to island diffusion. These predictions can be tested by HTD experiments on different Cu surfaces.

Diffusion coefficients for the surfaces Cu(1 0 0) [26], Cu(1 1 1) [41] and Pt(1 1 1) [42] at a temperature of 300 K are shown in Fig. 3.1. Most notable differences are the different monomer diffusion rates on surfaces, and the steeper descent of the island diffusion of the larger islands on (1 1 1) metals as compared to the Cu(1 0 0) case. The data span over limited range of island sizes, $s = 1 \ldots 10$ for Cu(1 1 1) and $s = 1 \ldots 7$ for Pt(1 1 1), and all the other island sizes are extrapolated [26]. The asymptotic behavior of the extrapolation approaches power law $D_s \sim s^{-1.2}$ at large

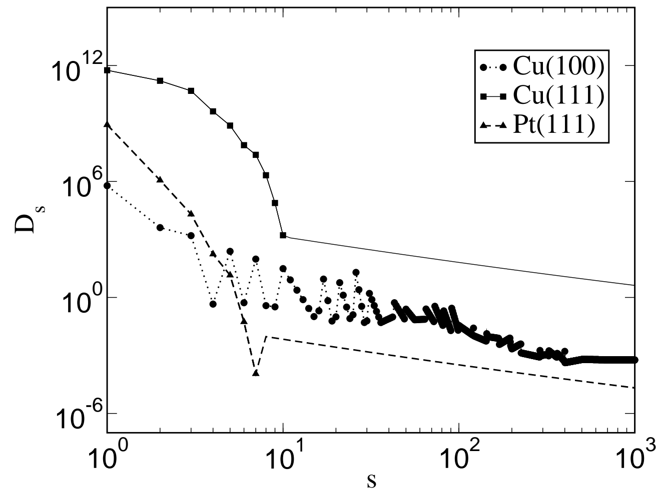

Figure 3.1: Diffusion coefficients for Cu(1 0 0) and Pt(1 1 1) at 300K as circles and triangles, respectively. The corresponding fitted continuation of the data for large island sizes are shown as solid and dashed lines for the Cu(1 1 1) and Pt(1 1 1) data. The dotted line is guide for the eye and follows the Cu(1 0 0) data.

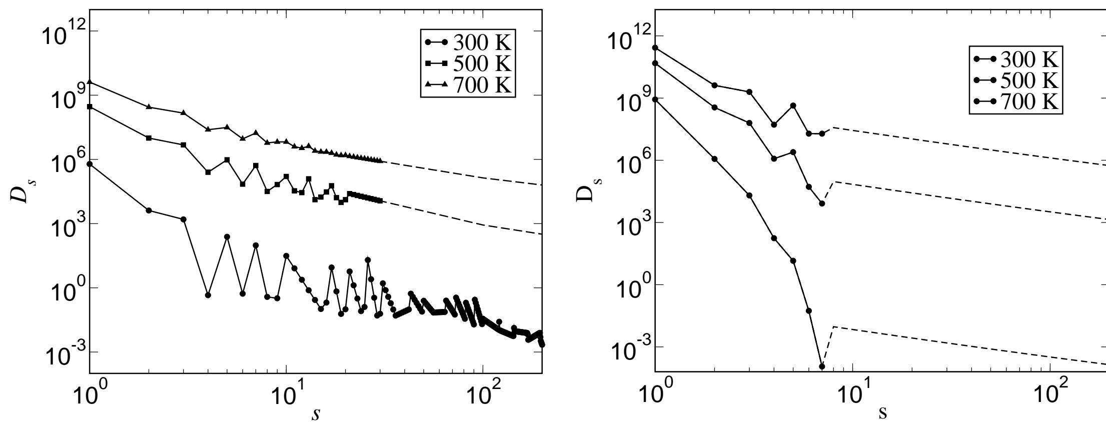

Figure 3.2: Diffusion coefficients for Cu(1 0 0) (on the left) and Pt(1 1 1) (on the right) at various temperatures.

s.

The diffusion coefficient for Cu(1 0 0) is shown in Fig. 3.2 (the left hand side panel) at temperatures 300 K, 500 K and 700 K. There was no need to extrapolate these data, but in some places there is linear interpolation on the log–log-scale applied, where certain island sizes were missing in the data [26]. The most important feature for Cu(1 0 0) is the oscillations of the diffusion coefficient due to almost immobile compact configurations that are present. The coefficients are obtained by Monte Carlo simulation using embedded atom method energetics [26].

The diffusion coefficient for Pt(1 1 1) is shown in Fig. 3.2 (the right hand side panel) at temperatures 300 K, 500 K and 700 K. We have extrapolated the data for $s > 7$ from Ref. [26]. Data are obtained from experiments using field ion microscopy [42]. The difference to the Cu(1 0 0) case is clear. The diffusion coefficient does not oscillate, but large islands become very rapidly almost immobile. Only at high temperatures there is indication of compact islands being slow, and at $s = 4$ there is a slight decrease of the diffusion rate.

The total flux of island density due to aggregation is

$$f_{a,s} = \frac{1}{2} \sum_{i+j=s} K(i,j) n_i n_j - \sum_{i=1}^{\infty} K(i,s) n_i n_s. \tag{3.5}$$

In this cases the aggregation kernel will be taken to be $K_{ij} = D_0(i^{-\mu} + j^{-\mu})$. This is a great simplification, and a Smoluchowski equation (3.1) with a kernel of this form has an analytical solution (See Reference [38] for details).

3.2.3 Island break-up

In reversible growth the islands break up into smaller parts during growth. This in effect broadens the island size distribution and slows down the growth. Particularly,

if only adatoms are allowed to detach from the large islands, the detached adatoms create an additional effective adatom flux which adds to the deposition and then gives rise to high adatom density. The flux of island density in Eq. (3.2) associated to the break-up is given by

$$f_{b,s} = \frac{1}{2} \sum_{i+j=s} F(i,j) n_{i+j} - \sum_{i=1}^{\infty} F(i,s) n_{s+i}. \tag{3.6}$$

The break-up kernel can be derived by taking into account that only monomers are allowed to detach

$$F(i,j) = F_0 (i+j)^{\alpha} (\delta_{1i} + \delta_{1j}), \tag{3.7}$$

where the Kronecker δ-symbols limit the break-up to single adatom detachment.

In HTD island growth proceeds reversibly through enhanced adatom detachment. The parameter α depends on the system. Assuming that the detachment rate is proportional to the perimeter of an island gives $\alpha = 1/2$. This is a justified choice for HTD, since with typical HTD conditions only adatoms, and not any larger units, are detached from islands. This notion has been also confirmed by recent MD simulations (See Paper II).

3.3 Rate equations for aggregation-detachment-recombination of islands and vacancies

The modeling of growth under IBAD conditions poses some additional challenges in comparison to modeling growth in LEID. In IBAD one must take into account the creation of vacancies and the effect of vacancies on island growth, as well as their clustering. Therefore, the processes of interest in the submonolayer regime of growth include:

1. Target adatom and vacancy defect production

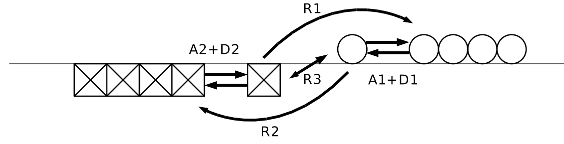

Figure 3.3: A schematic presentation of the relevant processes taking place during simulation of IBAD. Aggregation of adatoms to larger islands (A1) and detachment of adatoms from islands (D1) are accompanied by similar processes for single vacancies and vacancy islands (A2 for aggregation and D2 for detachment). The interlayer recombination processes R1, R2, and R3, represent the removal of single adatom from island by recombination with a single vacancy, filling up a vacancy island with a single adatom, and filling up a single vacancy with a single adatom, respectively.

2. Adatom and vacancy diffusion

3. Island diffusion

4. Detachment and breakup [11, 19, 22, 43] (See also Paper II)

5. Interlayer transitions between adatoms and vacancies [20]

Of these processes, we take into account here only those including single adatom or vacancy, thus excluding island break-up and island-island coalescence.

The basic atomistic processes during growth considered here are described schematically in Fig. 3.3. They all influence the time evolution of the adatom and vacancy island number densities n_s and n'_s, respectively, which are the fundamental variables in the Rate Equations (REs) given by

$$\begin{cases} \dot{n_s} = f_d + f_{a,s} + f_{f,s} + f_{r,s} \\ \dot{n'_s} = f'_d + f'_{a,s} + f'_{f,s} + f'_{r,s}. \end{cases} \tag{3.8}$$

For each quantity, the rate of change of the distribution equals the total fluxes f_i due to the basic atomistic processes. These fluxes are functions of the density variables and include f_d for deposition of adatoms on the surface, f_a for attachment of adatoms to islands, f_f for detachment of adatoms from islands, and f_r for interlayer recombination. In the second equation, the primes denote the corresponding fluxes for vacancies. In addition, the flux of deposited adatoms given by Φ monolayers per second (ML/s) and the flux of the ion bombardment set up the two other important experimental control parameters.

In what follows, the basic atomistic processes are described through the reaction rates and flux terms in a phenomenological and simplified form. Here it is enough to note that in principle the dependence of rates on the energetics and temperature follows activated Arrhenius behavior. For example, diffusion on open metallic surfaces and thus also the adatom attachment to island edge occurs with a rate $f_a \propto \exp(-E_D/k_B T)$, where E_D is the diffusion barrier. Similarly, the recombination rate is related to interlayer transitions occurring with rate $f_r \propto \exp(-E_{IL}/k_B T)$, where E_{IL} is the corresponding (effective) barrier for crossing a step edge downwards through a kink site. However, the detailed association of rates with different microscopic barriers is not essential for the present work. In what follows, we discuss each of these process in more detail and define the parametrization.

The rate of deposition Φ is expressed in ML/s. The rate of deposition for islands is given by

$$f_d = \Phi \delta_{1,s}. \tag{3.9}$$

The term $\delta_{1,s}$ explicitly limits the deposition to single adatoms only.

Similarly, for the vacancy creation

$$f'_d = \xi \Phi \delta_{1,s}, \tag{3.10}$$

where the prefactor ξ expresses the relative strength of the two flux terms and acts as an externally controllable variable.

The aggregation of islands is driven by adatom diffusion, and in IBAD in addition to this also island diffusion influences the aggregation rates [22, 43, 44]. In the case of metallic surfaces the diffusion coefficient for islands of size s can be taken to follow a simple power law [26]

$$D_s = K_0 s^{-\mu}. \tag{3.11}$$

A good choice for the exponent is $\mu = 2$, which is taken as a fixed model parameter in the following. The prefactor K_0 gives the scale for the aggregation relative to the deposition. A dimensionless parameter $R = K_0/\Phi$ is introduced to fix the relative strength of aggregation and deposition, and also acts as an external variable. The aggregation rate, as described by the aggregation kernel for islands of sizes i and j can be then written as

$$K_{ij} = (D_i + D_j)(\delta_{1i} + \delta_{1j} - \delta_{1i}\delta_{1j}), \tag{3.12}$$

which allows island-adatom processes only. Thus, the flux f_a due to aggregation for islands of size s is given by

$$f_a = \frac{1}{2} \sum_{i+j=s} K_{ij} n_i n_j - \sum_{i=1}^{\infty} K_{is} n_i n_s. \tag{3.13}$$

Similarly, for vacancies the flux f'_a due to aggregation is given by

$$f'_a = \frac{1}{2} \sum_{i+j=s} K_{ij} n'_i n'_j - \sum_{i=1}^{\infty} K_{is} n'_i n'_s. \tag{3.14}$$

Recombination takes place between islands and vacancies. Here it will be limited to the cases where a single adatom falls into a large vacancy island, and where a single vacancy gets filled from a larger island. Adatom-adatom and vacancy-vacancy dimer formations are also included.

The recombination kernel is of the same form as the aggregation kernel, but two more parameters need to be introduced here. The flux corresponding to the recombination can be now written as

$$f_r = \gamma(1+\xi_2)\left(\frac{1}{2}\sum_{i+j=s} K_{ij} n_i' n_j - \sum_{i=1}^{\infty} K_{is} n_i' n_s\right), \tag{3.15}$$

for adatom, and

$$f_r' = \gamma(1-\xi_2)\left(\frac{1}{2}\sum_{i+j=s} K_{ij} n_i n_j' - \sum_{i=1}^{\infty} K_{is} n_i n_s'\right), \tag{3.16}$$

for vacancies. The relative strength of recombination is controlled through γ. The relative strength of the recombination of adatoms to vacancy islands and recombination of single vacancies to islands is controlled through ξ_2, so that $\xi_2 > 0$ gives the latter process a lower rate.

The detachment of single adatoms from islands is the only relevant mechanism of island breakup for small metallic clusters (See Paper II). The probability of a single adatom to detach from an island is proportional to the length of the perimeter of a compact island, and therefore the detachment kernel can be given by

$$F_{ij} = F_0(i+j)^{\alpha}(\delta_{1i} + \delta_{1j}), \tag{3.17}$$

where the parameter $\alpha = \frac{1}{2}$ in the following to reflect the assumption of detachment from the edge of compact islands. The prefactor F_0 gives the scale of detachment relative to aggregation.

With this parametrization the adatom flux due to detachment is

$$f_f = -\frac{1}{2}\sum_{i+j=s} F_{ij} n_{i+j} + \sum_{i=1}^{\infty} F_{is} n_{i+s}, \tag{3.18}$$

and similarly for the vacancies

$$f_f' = -\frac{1}{2}\sum_{i+j=s} F_{ij} n_{i+j}' + \sum_{i=1}^{\infty} F_{is} n_{i+s}'. \tag{3.19}$$

3.4 Scaling in rate equations

In case of complex model with many parameters as in the present case, it is of importance to find a way to reduce the multitude of representations of the results. Simply giving results for different sets of parameters is of no use, because it rarely gives insight on the interesting regularities contained in the data. Fortunately, in many cases it is possible to summarize the representation of results by using suitable scaling procedures and by using scaled variables. It is possible to define scaling for these kind of growth models in the same way as for models with less complicated structure (i.e. coagulation), even though there is no guarantee that usual scaling type solutions to Eq. (3.8) exists. Growth may still have stationary phases of growth where the *effective* (approximate) scaling laws hold (See Paper I).

In the following we use the probability density that a randomly selected atom is contained in an island of size s, viz. $p_s(\theta) = sn_s(\theta)/\theta$. The average island size is defined as $\bar{s} = M_2/M_1$, where the kth moment of the distribution is given by $M_k = \sum_1^\infty s^k n_s(\theta)$. Now the scaling function is defined as

$$g(x) = \bar{s} p_s(\theta), \tag{3.20}$$

where $x = s/\bar{s}$ (See Paper I). In the scaling regime this function is independent of coverage and the parameters $R \equiv K_0/\Phi$ and $\kappa \equiv F_0/K_0$. It is possible to define scaling behavior for average island size as a function of coverage θ: $\bar{s} \propto \theta^\beta$, where the dynamic scaling exponent β is introduced. In model introduced it may be the case that the scaling does not appear to be valid. It is still possible to find such a regime for the model parameters that $\bar{s}$ is of power law form and that the data collapse for the scaling function is good.

We next assume the validity of the scaling forms for $\bar{s}$ and $g(x)$ and substitute these in the rate equations of Eq. (3.2). We obtain differential equations governing $\bar{s}$, the adatom density n_s and the average island density $N = \sum n_s$ [29]. By requir-

ing stationarity of the solutions, we obtain estimates for the dynamic and growth exponents in the limit in Eq. (3.2), where $s \to \infty$, $i \to \infty$ and $\bar{s} \to \infty$, so that $s/\bar{s} = \text{const.}$, and assume that all the integrals converge, we get (See Paper I and Ref. [40], Appendix A on page 53)

$$\beta = \frac{2}{1+\mu}, \quad \text{for } \theta \ll \theta_{\text{max}}; \tag{3.21}$$

$$\beta = \frac{1}{\mu+\alpha}, \quad \text{for } \theta \approx \theta_{\text{max}}. \tag{3.22}$$

Here θ_{max} represents the coverage where a maximum in the island density occurs. The limit $\theta \ll \theta_{\text{max}}$ corresponds to growth in the absence of detachment ($\kappa = 0$). In the region $\theta \approx \theta_{\text{max}}$ adatom detachment begins to govern growth because there are enough islands to provide a supply of detached adatoms exceeding the number of deposited atoms. In this case growth becomes independent of R and κ[1].

3.5 Method for solving the rate equations

In order to study in full detail the kinetics of island growth as described by Eqs. (3.2) and (3.8) and without invoking any additional assumptions concerning scaling or stationarity, we have simulated the submonolayer island growth using the Particle Coalescence Method (PCM). PCM has been used in solving wide range of rate equation problems and is a standard tool in the field [29, 40, 45–47]. In problems where the central interest is to acquire the average size distribution using rate equations, PCM is indispensable due to its effectiveness and flexibility. Compared to other numerical methods PCM avoids several difficulties. For stiff differential equations the solution is possible without further inconsistencies due to the discretization of equations for numerical integration. Also, the statistical errors are usually smaller

[1]The analytic predictions are assumed to be valid only for large values of $\bar{s}$ (or long times) and for $R \to \infty$. We have also numerically solved the differential equations for N and $\bar{s}$ and find that only when $1 \leq \mu \leq 3$ and $R \approx 10^{10} \ldots 10^{12}$ a power law type of behavior occurs, with good agreement with the analytic estimates. The slower steady state growth with β given by Eq. (3.22) is asymptotically approached when $\kappa R = F_0/\Phi \approx 10 - 100$.

in the average quantities of interest than those in the other methods, for example in KMC.

Even though it is possible to solve the RE models directly by numerical integration, it should be noted that the stiffness of the equations poses additional difficulties. The equations contain slowly and rapidly changing terms. Also, the conservation of mass is hard to attain in direct numerical integration. Additionally, the number of equations in the infinite set must be limited to a finite number for the numerical integration to be possible, and the discretization of the differential equations brings in the possibility to variable drift in the solutions, which can make the scaling analysis difficult. PCM avoids most of these problems. More details can be found in Ref. [40]

The basic idea in PCM is to treat islands as point-like objects, which is a good approximation at small coverages. Each island occupies only a single lattice site and aggregation and breakup occur with rates determined by the kernels $K_{i,j}$ and $F_{i,j}$, respectively. The definition of the reaction kernels is done as explained in the previous sections and is consistent with the computational scheme of PCM.

In this chapter the PCM computations have been performed mostly using a grid of 200×200 for the lattice size, and average quantities were calculated over 1000 individual runs of PCM integration, which proved to be enough for acquiring statistically significant island size distributions with a relative error below 3%. To verify the error estimates additional runs were done on a larger lattice (500×500) or with more repetitions (up to 2000 times).

3.6 Results

In this Thesis several aspects of HTD induced growth are discussed. The most notable new results focus on:

1. The transition to slow growth in IBAD;
2. The anomalously high adatom density observed in LEID;
3. The effects of adatom detachment on growth and calculation of the detachment probability using Molecular Dynamics;
4. The effects of diffusion on surface growth and islands size distributions on Cu(1 0 0) and Cu(1 1 1);
5. The properties of growth in IBAD when vacancies are formed on the surface due to the external ion bombardment.

3.6.1 Transition in the growth exponent of IBAD

In IBAD rich kinetic behavior occurs, as embodied in Eq. (3.2). For low detachment rates fast growth is found, which is associated with a large growth exponent β. As the relative strength of detachment is increased growth slows down and β decreases. Of particular interest here is the actual nature of the transition with increasing detachment rate in reversible growth from $\beta \approx 1$ to much slower growth with β determined by the exponents characterizing detachment and island diffusion. We suggest that this transition should be particularly clear when island diffusion is fast. In Fig. 3.4 we show the overall behavior of the dynamic exponent β as obtained from PCM simulations for various μ and α. In Fig. 3.4 we can see that when $1 \leq \kappa R \leq 100$ there is a sharp transition to qualitatively different type of growth characterized by

much smaller dynamic exponents $\beta \approx 0.45$ for $\alpha = 1/2$, and $\beta \approx 0.37$ for $\alpha = 1$. As expected, slower growth is obtained for enhanced detachment. Growth in this region where enhanced detachment dominates seems to be unexpectedly regular and the value of β does not depend on the rate κ after the transition.

3.6.2 Anomalously high adatom density in LEID

The scaling function $g(x)$ is compared in Fig. 3.5 with the experimental data of Degroote *et al.* [48] for growth with LEID where enhanced detachment is suggested to dominate the behavior of island size distributions. An anomalously high density of small islands was observed, in contrast to distribution obtained with thermal deposition.The agreement is remarkably good. In the experiments, it is estimated that $\kappa \approx 0.1$, but recent MD simulations of Co deposition on Ag indicate much lower values of $\kappa \approx 0.01$ (See Paper II). As the present results show, even such a low ratio of detachment to deposition is sufficient to lead to a high island density and maintain regular growth. Interestingly, the parameter region $\mu \approx 1.5-2$ with $10 \leq \kappa R \leq 100$ where regular growth occurs corresponds to those experimental parameters in LEID and other HTD techniques where layer-by-layer growth is observed.

PCM simulations show that with values of α close to 0.5 we will always have high adatom density, which is also the characteristic feature of experimental results. With significantly higher values of α the scaling of distributions in the submonolayer region is lost and approach to scaling form is very slow. Moreover, there is a tendency for extremely slow growth in time and a power-law type behavior of the of the scaling distribution for the small islands ($s \leq 10$) when $\alpha = 1$ is approached. On the other hand, with adatom detachment only, values significantly smaller than 0.5 will lead to higher values of the dynamic exponent β and thus to faster growth and with decreasing α the scaling function $g(x)$ rapidly begins to resemble the case for fragmentation. We can thus conclude that the enhanced adatom density really is a

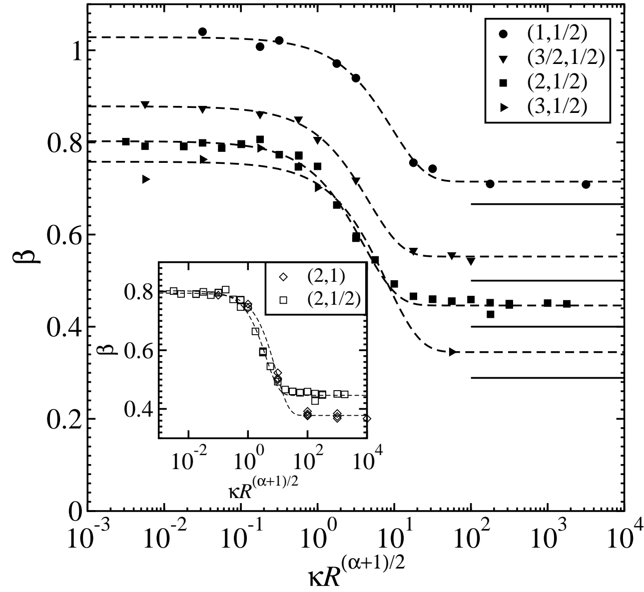

Figure 3.4: Growth exponent β for systems with $(\mu, \alpha) = (1, 1/2)$, $(3/2, 1/2)$, $(2, 1/2)$, $(3, 1/2)$ and $(2, 1)$ (inset) as a function of the parameter $\kappa R^{(\alpha+1)/2}$. Note the sharp transition to growth characterized by β given by Eq. (3.22) (solid lines).

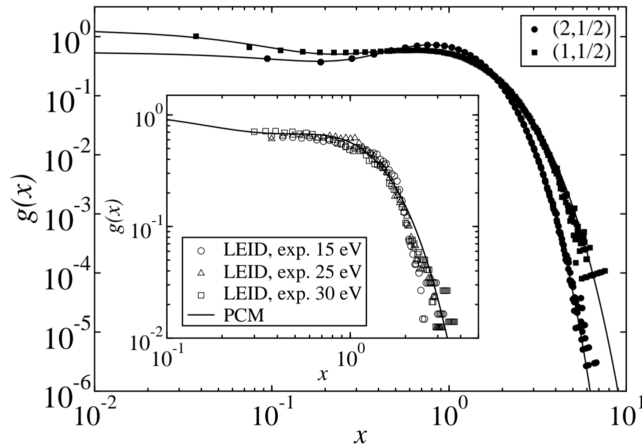

Figure 3.5: Fits to the simulation results for the scaling function (solid lines) and data for cases $(2, 1/2)$ (circles) and $(1, 1/2)$ (squares). In the inset the experimental data on LEID from Ref. [48] are compared with PCM simulations for $(2, 1/2)$.

characteristic feature related to detachment depending on the perimeter of island.

3.6.3 Detachment modeled using Molecular Dynamics

Our simulations (See Paper II) which correspond closely to the energy region of LEID applied in experiments by Degroote *et al.* [48] are conclusive with respect to the microscopic process; however, we cannot detect a single instance of island dissociation, and island fragmentation seems to be a relatively rare event also. Instead, the dominant mechanism is either the enhanced detachment of adatoms or several consecutive fragmentation/detachment events eventually leading to several detached adatoms. The total effect of these events is rather well described by a detachment kernel with $\alpha = 1/2$ (See Fig. 3.6). It is exactly this kind of kernel, which uniquely leads to a stationary, scaling form of island size distribution typical to LEID characterized by a high density of small islands.

3.6.4 Realistic diffusion rates for copper surfaces

The PCM simulations were carried out using realistic island diffusion coefficients discussed in Paper IV for Cu(1 0 0) and Cu(1 1 1), and with the detachment rate characterized by the exponent $\alpha = 1/2$. We define $\kappa = F_0/D_1$ and $R = D_1/\Phi$, where D_1 is the adatom diffusion coefficient. Parameters κ and R denote the importance of detachment relative to the diffusion, and of diffusion relative to the deposition flux, respectively. In the simulations the corresponding values were in the ranges $10^{-6} \leq \kappa \leq 10^{-1}$ and $10^5 \leq R \leq 10^9$. The simulations show that for large detachment rates, $\bar{s}$ and N indeed follow a power-law type of behavior, but as κ decreases, β becomes coverage dependent and saturates for $\kappa \to 0$ only as we have previously shown (Paper I). Thus, only for large κ can well-defined scaling exponents be extracted and regular island growth observed, and in this regime the island size distributions

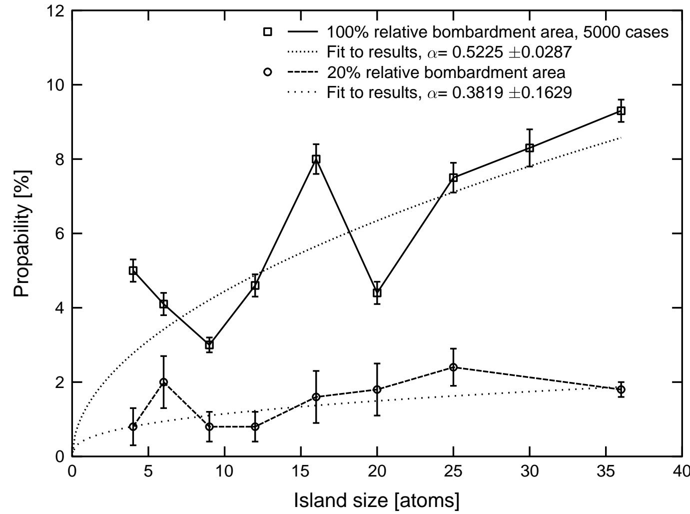

Figure 3.6: The detached Co atoms for the configuration with 100 % relative bombardment area (the area of irradiation of the surface was exactly of the area of the island under irradiation, so that 100% of the irradiating particles hit the island). A curve with a function of $F = Cs^{\alpha}$ has been fitted to the data, where C is a scaling factor and s the size of the island. The systems consisted of Co islands on Ag(1 1 1) bombarded by Co atoms.

are of scaling form.

The measured values of the dynamic growth exponent β at different temperatures and large κ both for Cu(100) and Cu(111) are shown in Table 3.1. The exponent β seems to be temperature dependent for Cu(100) but not for Cu(111). For Cu(100) this can be explained by examining the corresponding curves for the diffusion coefficients in Fig. 3.2. For small sizes (which is the case for large κ) the average slope of the diffusion coefficient curves depends strongly on temperature. If one fits a power law into the initial part of the data (for $s \leq 20$), the effective exponents are $\mu_{\text{eff}} \approx 5.4$, 3.6, and 2.8 at $T = 300$, 500, and 700 K, respectively. For the power-law type aggregation kernels we found (Paper I) that the dynamic exponent behaves as $\beta = 1/(\alpha + \mu)$, when $K(i, j) \propto i^{-\mu} + j^{-\mu}$. Using the effective exponents above this prediction gives $\beta \approx 0.17$, 0.24, and 0.30, showing a similar trend as the measured values from the PCM simulations. If the measured values are used, somewhat

T (K)	300	500	700
Cu(100)	0.25	0.34	0.43
Cu(111)	0.25	0.22	0.3*

Table 3.1: Dynamic scaling exponents β as defined in the text at different temperatures obtained from the PCM simulations, using the diffusion coefficients for Cu(100) and Cu(111) in Figs. 3.2 and 3.1. The asterisk for Cu(111) at $T = 700$ K indicates that the exponent is not yet constant in time. The errors in the other cases are about ± 0.05.

smaller values of μ_{eff} are obtained than from the fits to the diffusion coefficient data. If the fitting is done only through the maxima of the diffusion coefficient curves, better agreement is obtained. It is also interesting to note that $\bar{s}$ does not depend on R in this regime, but only on κ. This suggests that it could be possible to tune the regime for the effective diffusion exponent on Cu(100) by changing κ. However, this effect is probably too small to be seen, since e.g. on Cu(100) at $T = 300$ K we get $\bar{s} \approx 12$ atoms for $\kappa = 10^{-3}$, and $\bar{s} \approx 7$ atoms for $\kappa = 10^{-2}$, while the differences in β between these two cases are within the error bars. For Cu(111) there is no clear power-law for small sizes where the simulation data for diffusion coefficients exist. Instead, small islands seem to be rather mobile relative to adatoms in all temperatures.

We expect to observe scaling of island size distributions on the basis of the fact that well-defined scaling exponents exist for large detachment rates. In Fig. 3.7 we show scaled island size distributions in a modified form $g(x)$ (see Section 3.4) for large values of detachment rates using the diffusion coefficients for Cu(100) and Cu(111) shown in Figs. 3.2 and 3.1, and setting $\alpha = 1/2$, $R = 10^6$, and $\kappa = 10^{-2}$. On Cu(100) the data for different temperatures collapse to a single curve, and for $x < 1$ the scaled distribution is almost flat. Deviations between different temperatures occur at small sizes, which reflects the differences in the diffusion coefficients. The inset shows the scaled distribution on Cu(111). In this case scaling of the distribution is not as good,

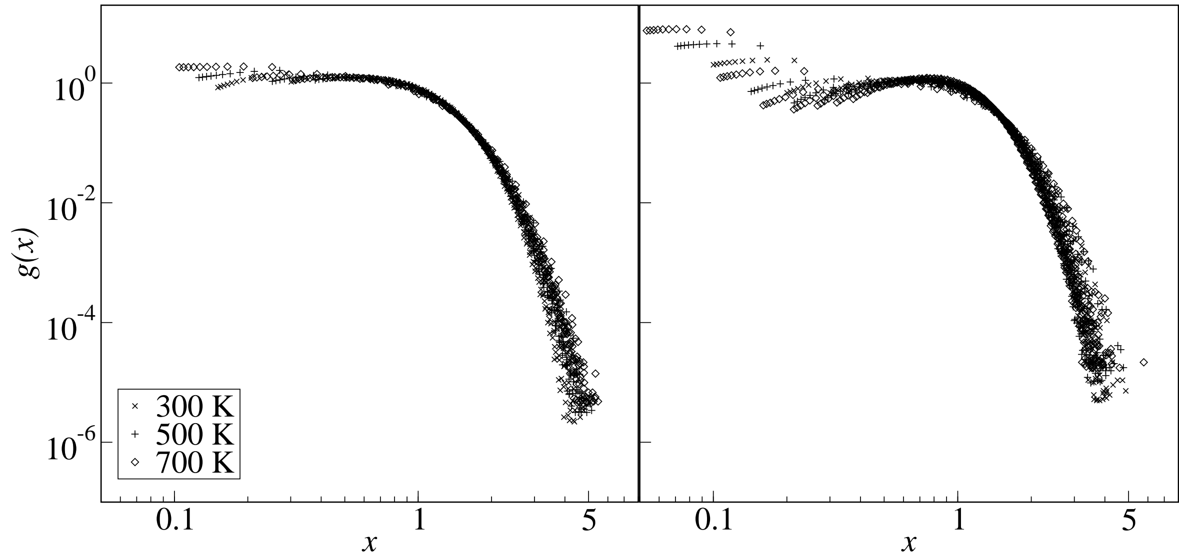

Figure 3.7: The scaled island size distributions $g(x)$ on Cu(100) as function of $x = s/\bar{s}$ (see Section 3.4). The different symbols correspond to $T = 300$ K (circles), $T = 500$ K (squares), and $T = 700$ K (triangles) with $R = 10^6$, $\kappa = 10^{-2}$, and $\theta \leq 0.25$ ML. The right panel shows the distributions on Cu(111) with the same parameters.

and differences at small sizes are larger than on Cu(100). It is, however, expected that deviations could be seen in the large size tail of the distribution. Since the diffusion coefficients rapidly decrease several orders in magnitude, as a function of the island size aggregation events leading to large sizes are basically between a small island and a large one.

3.6.5 Properties of growth in IBAD with vacancy creation

When the growth conditions in IBAD are such that surface vacancy creation must be taken into account we use Eq. (3.8) to model the growth and the additional vacancy-island recombination. We consider here three different cases, where the two central control parameters (R, κ) cover a range of values $(10^6, 10^{-4})$, $(10^5, 10^{-3})$ and $(10^4, 10^{-2})$ but where the product $\kappa R = 100$ is constant. These values have been chosen to make it possible to see the influence of the parameters R and κ on the scaling function and coverage dependence of the mean island size $\bar{s}$ for wide range of physically meaningful parameters.

In Fig. 3.8(a) we show the adatom and vacancy island size distributions as a function of island size for different recombination rates γ at the maximum simulated coverage of $\theta = 0.25$. The results in Fig. 3.8(b) demonstrate the basic qualitative behavior: steady growth of islands ($\gamma = 0.0$), slowed down growth ($\gamma = 0.6$) and terminated growth ($\gamma = 1.0$). In the last case the stationary island size is reached and the growth rates of vacancy and adatom islands are identical. The mean size of the vacancy islands is plotted as a function of coverage as the recombination rate γ changes. In this case the maximum size is reached at different stages of growth, and the coverage $\hat{\theta}$ where this happens is defined as the turning point (or the point of the inflection) of the curve. The quantity $\hat{\theta}$ at the turning point gets smaller as γ grows, and when $\gamma \to 1$, $\hat{\theta}$ attains values between 0.05 and 0.01, for ξ between 0.8 and 0.2, respectively.

The detailed dependence of the turnover coverage $\hat{\theta}$ on the different parameters defining the growth conditions is of central interest here to determine the optimum conditions of growth. However, before this we need to know whether or not the general behavior of the size distributions is of scaling form. For certain combination of values for the external control parameters discussed here, namely ξ, γ, ξ_2, we find that island size distribution scales according to Eq. (3.20) and furthermore, the general behavior of the scaling function is qualitatively similar in all cases studied.

First, the scaling function $g(x)$ of the size distribution is coverage independent in the case where island deposition is equal to vacancy creation ($\xi = 1$), and no recombination occurs ($\gamma = 0$) (see Fig. 3.9). There is a high number density of small islands up to the mean island size, while for sizes larger than the mean size the number density decays quickly. The exact form of the function depends slightly on the control parameters, but retains the general form discussed above for a wide regime in the external parameters. This means that the properties of growth as contained in the scaled distributions are relatively robust and not very sensitive to changes in the external conditions. It should be noted, however, that the recombination process ($\gamma > 0$) explicitly breaks the scaling of the vacancy island size distributions, which become strongly coverage dependent whenever the rate of vacancy creation is slower than the deposition flux of adatoms $\xi < 1$. In this case the scaling function for the islands still retains scaling form quite well if $\xi \lesssim 0.8$, i.e. vacancy creation is sufficiently slow as compared to deposition of new adatoms on the surface.

Finally, strong recombination in the case of equal deposition and vacancy creation leads to a stationary state, where the mean island size ceases to grow, and both the scaled island and vacancy size distributions become coverage dependent. The main result here is that the scaled form of the size distributions is very similar in a wide range of parameter values. Therefore, it is enough to concentrate on the behavior of the mean size. This greatly simplifies the determination of the range of parameters, where optimally smooth growth can be obtained. To this end, we just need to know

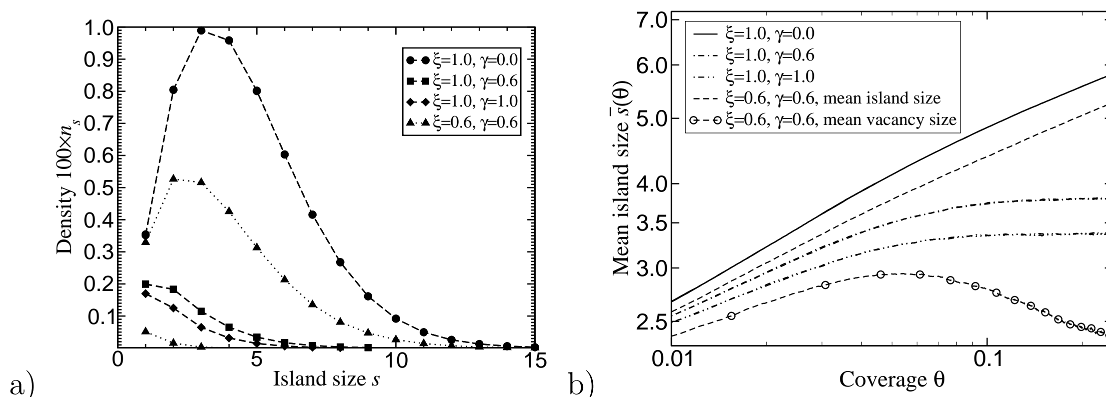

Figure 3.8: (a) The island size distribution function for different cases: no recombination and equal deposition of adatoms and creation of vacancies (solid discs), added recombination ($\gamma = 0.6$) (solid squares), and added strong recombination ($\gamma = 1.0$). The upper dotted line with solid triangles shows the island size distribution function and the lower one the vacancy size distribution function. For all shown cases $\theta = 0.25$.
(b) The mean island size $\bar{s}$ as a function of coverage θ is plotted for the cases in (a) (see legend for details). The case shown has $(R, \kappa) = (10^5, 10^{-3})$.

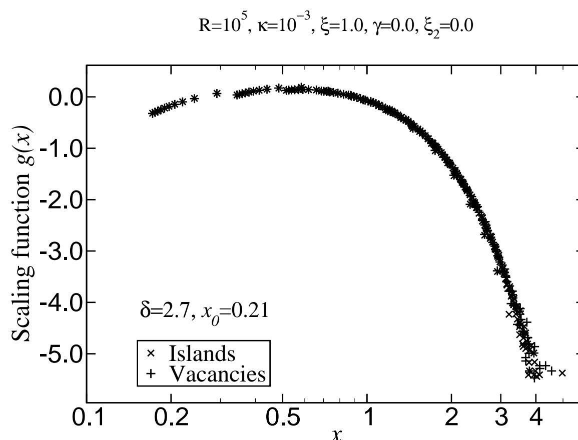

Figure 3.9: Scaled island size distributions for adatoms and vacancies. The functional form $g(x) \sim x^\delta \exp(-x/x_0)$ can be fitted to the shown data.

Table 3.2: The effective growth exponent $\tilde{\beta}$ for adatom islands in the case with $(R,\kappa) = (10^5, 10^{-3})$ tabulated against selected combinations of the parameters ξ and γ.

ξ	1.0	1.0	1.0	0.6	1.0	1.0	1.0
γ	0.0	0.6	1.0	0.6	0.2	0.6	0.8
ξ_2	0.0	0.0	0.0	0.0	0.6	0.6	0.2
$\tilde{\beta}$	0.359	0.206	0.119	0.330	0.270	0.183	0.133
$\tilde{\beta}'$					0.356	0.272	0.164

Table 3.3: The fitting parameters Γ_s and Γ_θ for symmetric recombination (upper panel), and asymmetric recombination with $\xi_2 = 0.5$ (lower panel).

(R,κ)	$(10^4, 10^{-2})$	$(10^5, 10^{-3})$	$(10^6, 10^{-4})$	$(10^5, 10^{-3})$
ξ_2	0.0	0.0	0.0	0.5
Γ_s	0.143(6)	0.35(1)	1.02(7)	0.40(1)
Γ_θ	1.02(8)	1.73(6)	2.87(8)	1.6(1)

the dependence of the turnover coverage $\hat{\theta}$ on the different parameters defining the growth conditions as well as the effective growth exponent[2] $\tilde{\beta}$ of the mean size before $\hat{\theta}$. The values for $\tilde{\beta}$ are listed in Table 3.2 for several representative cases, and are seen to stay between $\tilde{\beta} = 0.12 \ldots 0.36$ for wide range of parameters.

Fig. 3.10 shows the dependence of the maximum vacancy island size as a function of γ for different values of ξ varying from 0.2 to 1.0. It is interesting to note that the different curves representing the behavior of the maximum island size can be

[2]In this part the growth exponent β has been replaced with an effective growth exponent $\tilde{\beta}$ due to the approximative nature of the scaling. The effective growth exponent has been measured at single coverage by fitting a powerlaw to the mean islands size as a function of coverage.

collapsed to a single curve by using the fitting formula

$$\bar{s}'_{\max} = S_0 \exp(-\Gamma_s \gamma), \tag{3.23}$$

where the prefactor can be fitted with a linear dependence on ξ as $S_0 \propto \xi + \xi_0$, and where ξ_0 depends on (R, κ). In Table 3.3 we list the values of the fitting parameters for the various cases studied here. Similarly, we find that the coverage $\hat{\theta}$ at the maximum mean vacancy island size can be fitted by using the expression

$$\hat{\theta} = \Theta_0 \exp(-\Gamma_\theta \gamma), \tag{3.24}$$

with values of the fitting parameters again given in Table 3.3. The values of the parameter needed to calculate the crucial quantities in determining the optimum region of growth are now all known for a wide range of control parameters. However, there does not seem to be a singe well defined and regular dependence of these parameters on the combination (R, κ), or κR.

The asymmetry of the recombination is probably the most common case in practice, due to the presence of the Ehrlich–Schwoebel barrier in metallic films, and this considerably complicates the problem. However, the results we have obtained suggest that the asymmetry only affects the quantitative behavior but not the qualitative features of growth. This somewhat unexpected behavior is demonstrated in Fig. 3.11(b), where the mean island size is shown for different asymmetries, and in Fig. 3.11(a), where typical island size distributions are shown. As is evident in these figures, the general behavior remains the same as in the case of symmetric recombination. Fig. 3.11 omits the case of unequal deposition of adatoms and creation of single vacancies, but similar behavior occurs as is shown in Fig. 3.8 for the symmetric deposition-creation case, as the asymmetry in recombination gives only a small variation to the turning point and the maximum vacancy size. The general properties of the growth are independent of the recombination asymmetry ξ_2.

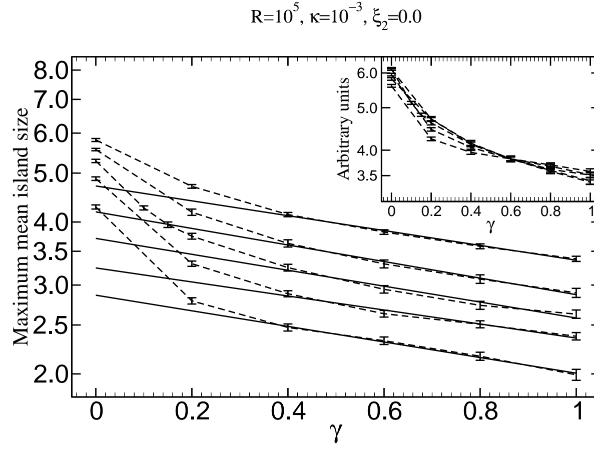

Figure 3.10: The maximum island size $\bar{s}'_{\text{max}}$ for vacancy islands as function of γ, for $\xi = 0.2$, 0.4, 0.6, 0.8 and 1.0 (from bottom to top). In the inset we show the data collapse (see text for details).

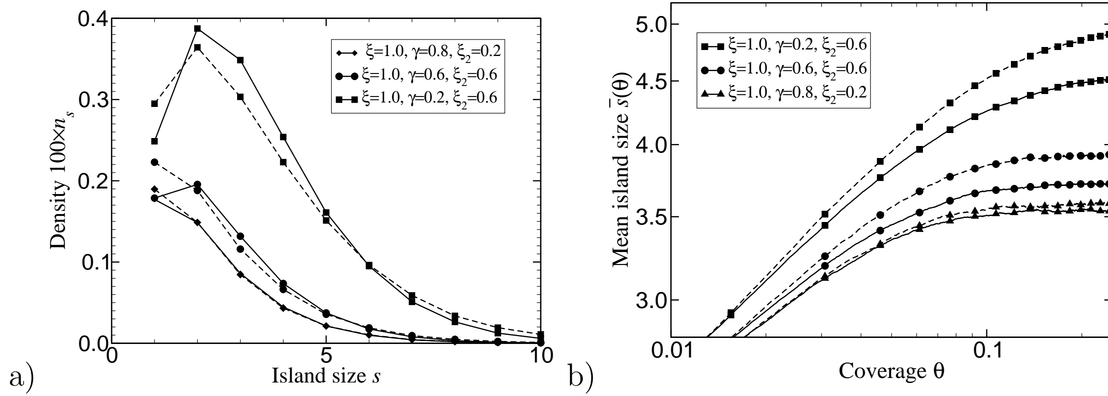

Figure 3.11: (a) The island size distribution function (solid line) and vacancy island size distribution function (dashed line) in selected cases (see legend for details). (b) The mean island size $\bar{s}$ as a function of coverage θ corresponding to the cases in (a) (see legend for details). Both figures show data for $(R, \kappa) = (10^5, 10^{-3})$.

3.7 Conclusions on submonolayer growth

A particularly striking observation made in the LEID experiments is that with different deposition energies an anomalously high density of small islands is observed, with the scaled distribution function behaving as $f(x) \sim 1/x$ for $x < 1$ [11]). We have shown using the rate equation approach (See Paper I) that this anomalously high density of small islands is due to a balance between island–island aggregation and enhanced adatom detachment. The effect of ion bombardment induced detachment has been studied using Molecular Dynamics simulation, which has confirmed the physical assumptions behind the basic rate equation model (Paper II).

Several atomistic processes have been suggested as an explanation for the observation that by using LEID layer-by-layer growth can be either promoted or sustained in systems, which otherwise would grow in the 3D growth mode. At low bombarding energies of order 50 eV or smaller the effect of ion bombardment is to increase detachment, and thus to increase the density of small islands [11, 19, 49] as well as to increase the step density [15]. In addition, surface defects in form of surface adatom and vacancy pairs are formed, and this redistribution of surface atoms due to impacts of the energetic ions helps to increase the adatom concentration (wetting), and thus leads to nucleation of new islands [49, 50]. Finally, energetic ion impacts also substantiate interlayer mass transport processes, leading to enhanced downward mass transfer, which tends to relax the surface corrugations [15, 19, 20].

One of the most important questions that still remains open is the role of *island* diffusion, since for mobile islands the aggregation rates in the RE approach depend explicitly on the diffusion coefficients D_s of islands of different sizes s. Island diffusion on surfaces has been studied both theoretically [26, 51, 52] and experimentally [42, 53–59]. While in the large island limit the size dependence of the island diffusion coefficients can be classified based on simple basic processes [60, 61], for smaller islands D_s depends on the geometric and energetic details of the underlying surface,

and can be a complicated, non-monotonic function of s [62–66]. To this end we have studied the effect of diffusion using realistic diffusion coefficients on Cu(1 0 0) and Cu(1 1 1) (see Paper IV).

Kyuno and Ehrlich [42] have studied surface growth in a model where they include cluster dissociation. Their results show that the dissociation effect will be the most important factor affecting island growth, and they conclude that island mobility is of minor concern in this context. However, their results concentrate on such average quantities that are expected to be unaffected, and they do not consider the island size distribution or the dynamic growth exponent β. In our work we have shown that the island mobility has a significant effect on these quantities.

In order to construct realistic REs it is necessary to find proper rate coefficients describing the various processes in the REs. This has been accomplished successfully in the case of growth with immobile island and adatom detachment [67, 68], and a self-consistent formulation of this problem has been given [67]. However, in this Thesis we have shown that it is sufficient to formulate phenomenological rate coefficients by considering their microscopic origins only at a depth, which is required to obtain correct *qualitative behavior* of the growth.

In this chapter we have also described a rate equation model for submonolayer growth in a situation where the flux of adatoms coming on the surface creates surface vacancies. Diffusion of these adatoms and single vacancies leads to island formation for both. Recombination process between adatoms and surface vacancy islands, and also between single surface vacancies and adatom islands, have been included in the model. The rate equations have been solved using the Particle Coalescence Method to obtain the relevant size distributions for the adatom and vacancy islands as a function of the coverage. The results of this model are comparable to the findings of ion bombardment experiments on Ir(1 1 1) [21], and the model is in qualitative agreement with the available experimental results. In their conclusions

in Ref. [21] Petersen *et al.* state that efficient surface diffusion in the absence of bulk vacancy cluster diffusion leads to a pure growth morphology consisting only of adatom islands. This is realised in our calculation in the case where the vacancy creation rate is sufficiently lower than the adatom deposition. They also state that inefficient surface diffusion leads to a morphology representing adatom islands as well as vacancy islands. This is realised in our model by supressing the interlayer recombination, which is connected directly to the diffusion rates of islands and vacancy islands.

4 From Submonolayer to Multilayer growth

The submonolayer growth studied in LEID and IBAD in this Thesis is of course only the initial stage of growth, and favorable conditions needed to maintain the high density of islands as well as sufficiently effective annealing of surface defects are prerequisites for successful multilayer growth. Therefore, a controlled multilayer deposition method demands that the layer-by-layer growth mode is attained and can be controlled to the degree that growth instabilities can be suppressed. The most important stage is maintaining the layer-by-layer mode as long as possible before the second layer starts to nucleate. The analysis of submonolayer growth in the previous chapters completes the study of phenomenology of first layer growth. The layer-by-layer growth mode can be maintained if the ion bombardment energy is in the optimal range (Paper VI). The IBAD and LEID methods of deposition can thus be used to control the onset of second layer nucleation, which is possible only if large islands are created in the early stages of first layer growth.

This means that the island edge Ehrlich–Schwoebel barrier must be overcome. IBAD does this by adding external ion bombardment to break up large islands and give the already nucleated islands on the second layer excess energy to hop off the island. In LEID the incoming ion flux causes the islands to stay small, and thus prevents the second layer nucleation altogether by inducing adatom detachment, which adds to the small island nucleation on the substrate layer. Further, low energy ion deposition is frequently used to maintain or promote smooth epitaxial growth of thin films. In LEID energetic ion beams with ion energies ranging from a few eV up to a few tens of eV are used to prevent the onset of 3D growth mode and to keep the surface in 2D layer-by-layer growth mode. Thus layers with improved smoothness are obtained (see e.g. references [11, 43, 48, 69] and references therein).

We have determined optimum conditions for submonolayer nanoisland growth in

IBAD. This situation, which is characterized by the onset of smooth layer-by-layer growth requires knowledge of the borderline case, where vacancy islands begin to be filled. When ion bombardment is more moderate than in this borderline case, there is no significant erosion of the surface and IBAD is useful in maintaining or facilitating smooth layer-by-layer growth. Before this borderline case is reached, there is steady growth of adatom and vacancy islands, and during this stage of growth the properties of growth are well described by scaling solutions for the mean size, and a well-defined scaling exponent. However, the smaller the critical coverage below which this region of steady growth takes place, the sooner the vacancy islands start to fill and shrink away, and the more advantageous IBAD is in maintaining the desired layer-by-layer growth. Also, the mean size of the islands remains small enough in this case preventing the onset of second layer nucleation and roughening of the surface. Therefore, knowledge obtained in the present study about the critical size and the maximum island size and how they depend on the values of the control parameters should be useful in tailoring growth through ion-assisted deposition.

The effects of microscopic processes on observable features of growth are now more or less known and understood on the microscopic level of description and can be approached by using molecular dynamics (MD) and kinetic Monte Carlo (KMC) simulation methods [15, 19, 20, 49, 50], but nevertheless it has been difficult to pin down general features of growth, which could be directly detected in experiments. The experimental results often report detailed visualizations of surface morphologies based on surface scanning probe microscopy [70], which give detailed microscopic information to be compared with microscopic MD and KMC simulations. However, these kind of microscopic studies are not easily adapted in making predictions on how the growth mode changes when the parameters determining the growth conditions are changed. Another class of experimental methods is based on monitoring the surface growth by electron scattering techniques such as LEED [71], RHEED [72, 73] or TEAS [73]. These methods yield information of the average properties of growth, such as the step density and surface roughness, and the growth mode can be detected

through the intensity oscillations on the reflected beam. In this case the overall features of the intensity variation can be related to the surface morphology, but the challenge is to connect the measured properties with model predictions.

In order to overcome the difficulties of bridging the model calculations with observable features of growth, a simple but realistic surface growth models are needed for such comparisons. MD and KMC simulations (see e.g. [15, 19, 20, 49, 50]) as well as the reaction kinetic models [23, 74–76]) used to describe surface growth are both aimed at describing the pertinent microscopic processes as accurately as possible, and consequently contain many parameters in the form of energy barriers or reaction rates related to microscopic processes (in KMC), or detailed and complicated two particle interaction potential using numerous parameters tuned for particular system in hand (MD). However, for most practical applications MD and KMC are too demanding and time consuming methods, and even the more coarse-grained RE descriptions may turn to to be computationally unfeasible or too cumbersome for practical cases. Therefore, simple phenomenological models are needed to bridge the gap between experimental results and modeling. What is required of this kind of phenomenological model is the capability to effectively compress the essential information of growth in a small enough set of parameters in a way that they can be connected to experimentally observable features of the growth. A suitable starting point for this is phenomenological modeling based on the description of time evolution of the total coverage of multiple layers, affected by the adatom current due to interlayer mass transport [77–79].

In Paper VI we have proposed a simple model for describing the layer-by-layer growth. Instead of time development of adatom and island concentrations, the model keeps track only of the total coverage of each layer. The model is closely related to total coverage models previously introduced in Refs. [77–79] for simplified description of layer-by-layer growth. In Paper VI it is also demonstrated how the model is used to quantify the properties of growth and changes in the growth mode,

which are measurable through LEED [71], RHEED [72, 73] or TEAS [73].

In modeling layer-by-layer growth in LEID the processes of interest are [23, 43, 75, 76]:

1. Target adatom and defect production
2. Adatom and defect diffusion, and island diffusion
3. Detachment of adatoms from islands and island break-up
4. Interlayer atomistic processes

Of these processes we concentrate here only on the interlayer mass transport, because for low energy ion bombardment in energy region up to a few tens of electron volts only the effective mass flow from layer to layer is of interest [15, 19, 20]. Of course, other processes also affect the growth within each layer (intralayer growth) and in particular the scaling behavior of island size distributions in each layer. Nevertheless, it seems that many details of intralayer growth can be ignored in cases of multilayer layer-by-layer growth, where the processes of most interest are ion bombardment induced *insertion of adatoms* from the upper layer to the edges of descending layers, and bombardment induced *pile-up events of adatoms* on the ascending layers [15, 19, 20].

The probability that the deposited adatom makes the downward jump due to the insertion event is denoted by p_-, while the probability for the upward jump by pile-up event is given by p_+. These both are purely kinematic effects due to ion impacts. It should be noted, that at thermal energies there is the low probability $p_{0+} \ll p_+$ of attachment to ascending terrace edge, generating an effective upward current [80]. Similarly, there is the downward current due to downward funnelling effect, occurring with probability $p_{0-} < p_{0+} \ll p_\pm$ [81]. These total relative probabilities

of downward insertions and upward pile-ups is shown schematically in the Fig. 1, where also is shown the ratio γ of probability $p_- + p_{0-}$ of pile-ups to $p_+ + p_{0+}$ of insertions. The parameter $\gamma = (p_+ + p_{0+})/(p_- + p_{0-})$ thus gives the ratio of upward to downward transition probability, and can be taken as the effective (normalised and dimensionless) mass transfer rate in our model.

In principle, the mass transfer rate depends also on the step densities on lower and upper terraces. In order to take this into account, we first assume that on the terrace k the step density is given by ρ_k, and on lower terrace $k-1$ ρ_{k-1}. Second, the total mass transfer rate either upwards (+) or downwards (−) are coupled with these step densities, which leads to the total mass transfer rate given by

$$\Gamma_k = \frac{(p_+ + p_{0+})\rho_k - (p_- + p_{0-})\rho_{k-1}}{(p_+ + p_{0+})\rho_k + (p_- + p_{0-})\rho_{k-1}} = \frac{\gamma R_k - 1}{\gamma R_k + 1}. \tag{4.1}$$

The definition of Γ_k is chosen to conform with the definition given by Fu and Wagner [79], but now with $\Gamma_k > 0$ for up step and $\Gamma_k < 0$ for down step mass transfer. In addition, we have the factor $R_k = \rho_k/\rho_{k-1}$, which takes into account the difference in step densities. Therefore, we need a model for step densities at different layers. According to the MD and KMC simulations of low energy ion bombardment, the step density of growing layers are nearly independent of the total deposition flux, and after the initial transient stage lasting up to partial coverage $\theta_c \approx 0.2$ ML it attains a constant value [15, 20]. An appropriate simplified description of the step density ratio is

$$R_k = \frac{\rho_k}{\rho_{k-1}} = \frac{1 - e^{-\theta_k/\theta_c}}{1 - e^{-\theta_{k-1}/\theta_c}}, \tag{4.2}$$

where θ_k is the fractional coverage of the layer k to be calculated from the model. However, for most cases the value $R_k = 1$ is appropriate (as will be shown later on) in which case the model contains only one parameter $\Gamma = \Gamma_k$ for all layers k. The values $-1 \leq \Gamma < 0$ correspond to effective mass flux downwards and $0 < \Gamma_k \leq 1$ upwards. The special case $\Gamma_k = 0$ corresponds to perfect simultaneous multilayer (SM) growth model, while $\Gamma_k = -1$ is the ideal layer-by-layer growth model and $\Gamma_k = 1$ is the ideal island growth model.

The kinetic equations for the growth of layers is now obtained by simply considering the contributions of deposition on a given terrace and mass currents from other terraces due to interlayer transitions. Following the model prosed by Fu and Wagner [79], we make the following simplifying assumption on the total mass currents. *Down-step diffusion* is described by processes, where adatom flow on terrace k is simply determined by the amount of available mass above the kth layer, given by the total flux J of adatoms entering onto the layer and the exposed surface area θ_k above the layer k, and in addition to this, by the uncovered area $\theta_{k-1} - \theta_k$ of the kth terrace itself. The decrease of the coverage of the kth level is similarly given by the product of the adatom flux $J(\theta_{k-1} - \theta_k)$ on it and the available uncovered area $1 - \theta_{k-1}$ below it. The rate coefficients of the adatom flux onto terrace k and out of it are given by Γ_k and Γ_{k-1}, respectively. *Up-step diffusion* is described by similar processes, where adatom flow on the kth terrace is given by the product of the total flux $J(1 - \theta_k)$ and the uncovered area $\theta_{k-1} - \theta_k$. The decrease of coverage of the kth terrace is given by the product of the flux $J_k(\theta_{k-1} - \theta_k)$ and the available uncovered area θ_k. Rearranging the terms we obtain kinetic equations of the form

$$\begin{aligned} \frac{d\theta_1}{dt} &= J(1-\theta_1)[1-\Gamma_1\theta_1]; \\ \frac{d\theta_k}{dt} &= J(\theta_{k-1}-\theta_k)[1-\Gamma_k\theta_k+\Gamma_{k-1}(1-\theta_{k-1})]. \end{aligned} \tag{4.3}$$

In comparing our model as given by Eq. (4.3) with the model of Ref. [79] the main difference is the generalization to layer dependent rate coefficients in terms of Eqs. (4.1) and (4.2), which now allows us to make the connection to microscopic atomistic process. The form of the equations is simple and easily solved for θ_k. However, their solutions for coverages θ_k are as such of little of help in quantifying the degree of layer-by-layer growth in a way which is experimentally easy to access. In order to have a convenient and flexible measure we need to relate the results of such calculations to experimentally measurable observables.

The evolution equations for growth in Eq. (4.3) are solved numerically for different values of parameters γ and θ_c. In Fig. 4.1 we show three typical cases: First,

when the downward transition dominates and γ is small enough the growth mode is typically of layer-by-layer type, detected also by the scattering intensity, which is of oscillatory type. The anti-phase scattering intensity can be expressed in terms of coverages and is given by $I = \left[\sum_{k=0}^{\infty}(-1)^k(\theta_k - \theta_{k+1})\right]^2$ [20, 82, 83]. This is shown in the topmost part in Fig. 4.1 where $\gamma = 0.01$. When the probability of pile-ups begins to increase and the mass transfer rate reaches values of order of $\gamma \approx 0.2$ the growth mode begins to change to simultaneous multilayer growth, indicated by decay of the maximum value in the intensity oscillations as shown in Fig. 4.1. Finally, at large enough values of $\gamma \approx 1$ the growth mode is of 3D type growth resulting in rough surfaces. In this region the scattering intensity decays rapidly with increasing number of completed layers.

The scattering intensity is a rather sensitive indicator of the growth mode. The onset of layer-by-layer growth is indicated by the oscillatory behavior of the intensity. Moreover, the decay rate of the intensity peaks can be correlated with the growth mode and used as a quantitative measure for the degree of layer-by-layer growth. The more perfect is the layer-by-layer mode the less the intensity decreases with increasing number of deposited layers. Therefore, by tracking the intensity maxima it becomes possible to quantify the degree of layer-by-layer growth. In Fig. 4.2 we show the dependence of the intensity decay on the model parameter γ governing the interlayer mass transfer. From the results shown in Fig. 4.2 it is seen that the decay of the intensity maxima follows a inverse power-law of the type $I \propto k^{-\beta}$, with a well defined decay exponent β. It is of interest to note that this behaviour is probably of general validity and not only a consequence of the simplifications within the model.

The relationship demonstrated here opens up a way to quantify the degree of layer-by-layer growth in terms of a single parameter directly related to the atomistic events caused by ion bombardment. The optimum window of bombarding energies predicted by the model for layer-by-layer growth in LEID is from 5 eV to 25 eV,

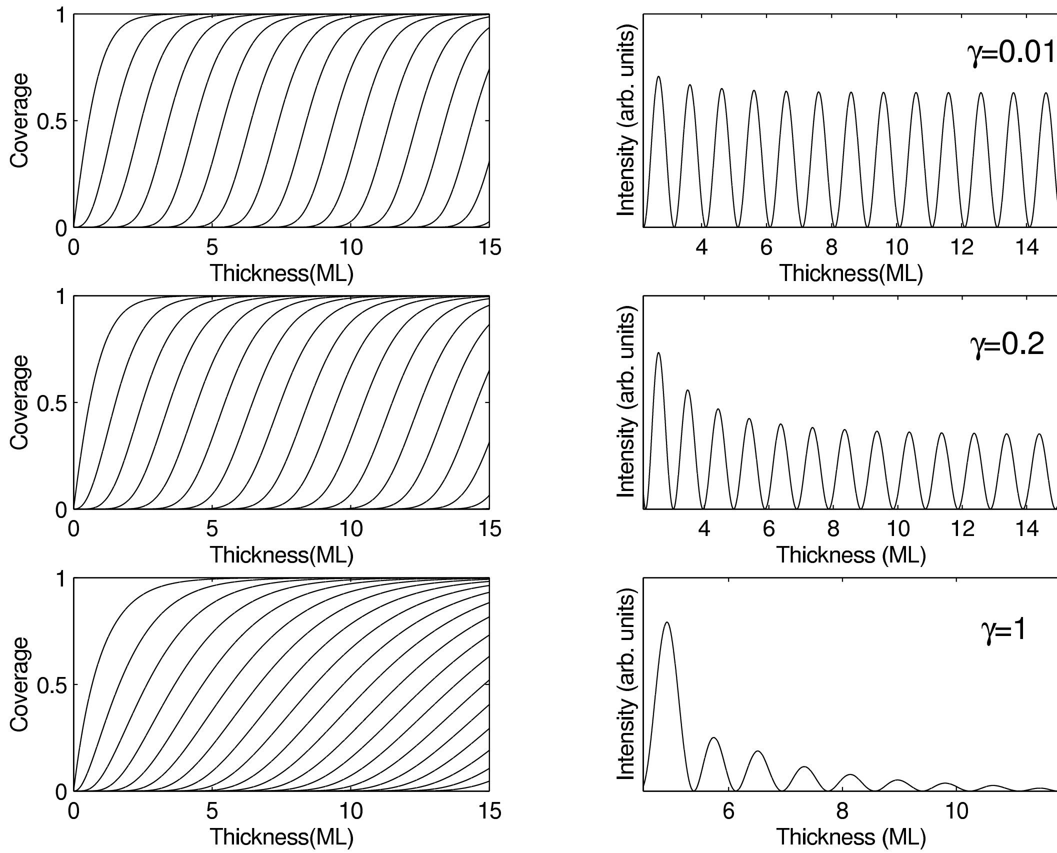

Figure 4.1: The evolution of the coverages θ_k (left panel) and the scattering intensity I (right panel) as a function of total coverage (ML). The results for $\gamma = 0.01$ (ideal layer-by-layer growth), $\gamma = 0.2$ (simultaneous multilayer growth), and for $\gamma = 1$ (rough 3D growth) are shown from top to bottom.

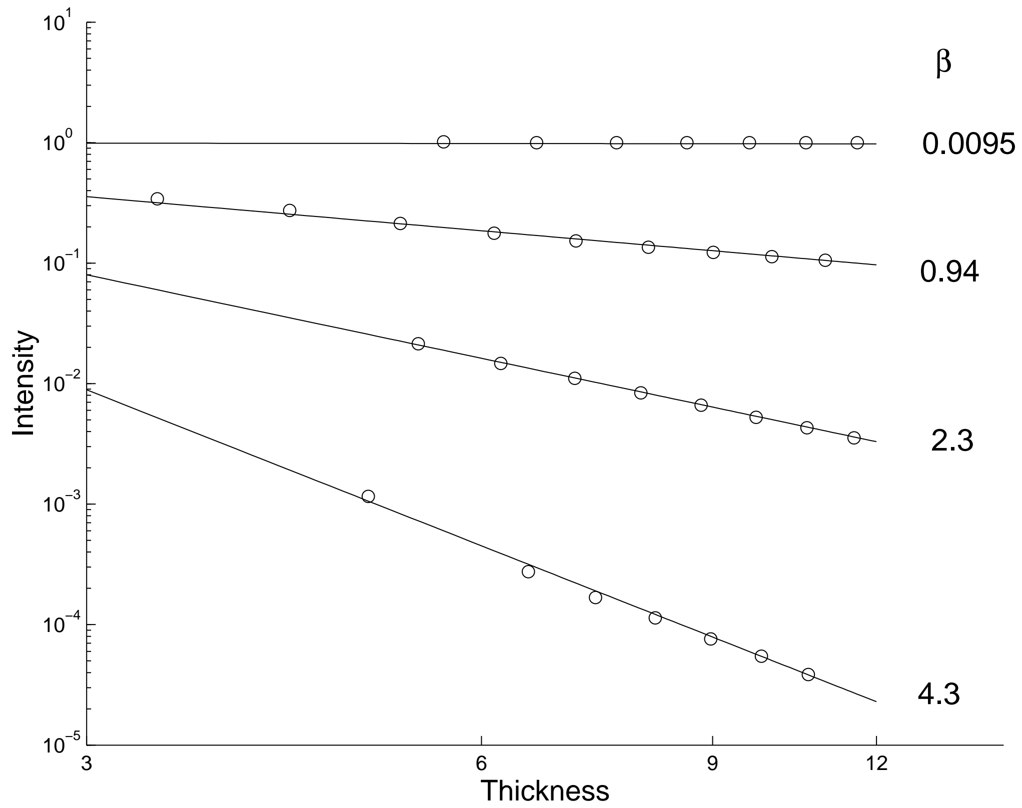

Figure 4.2: The Intensity maxima at different completed layers for $\gamma = 0.01$, 0.5, 0.8 and 1 from top to bottom. The fits of form $I \propto k^{-\beta}$ and the corresponding exponents β are shown. Results are given for $\theta_c = 0.2$.

which is in reasonable agreement with MD and KMC simulation results reported previously in the corresponding cases. Agreement with more detailed atomistic simulations supports the view that the phenomenological model discussed here is a reliable enough simplification for description of qualitative aspects of LEID on thin film growth. Although this kind of model cannot replace the more detailed simulations it may have owing to its simplicity many uses in practical situations for characterizing growth.

The model utilized is a simplified phenomenological model. A complete treatment of multilayer growth including all the effects which turned out to be intractable in submonolayer growth still poses a formidable computational problem even for the simplified RE description. Nevertheless the results presented here solve several problems in describing epitaxial growth in IBAD and LEID, pin down the region where such methods can be expected to be useful, and finally point out remaining problems and possible future directions for their solutions.

5 Summary and discussion

The approach in this Thesis has been to start with the most easily accessible phenomena in the submonolayer region, first trying to pin down how basic atomistic phenomena are reflected on experimentally measurable properties of the systems, on the level of size distributions and their scaling properties. One clear characteristic feature is shown to be the anomalously high small island density, which is related to adatom detachment from islands. The second one is the scaling of the island size distribution and the corresponding dynamic exponent related to island diffusion. The third is the borderline separating the island growth and erosion in IBAD, which is related to vacancy production and recombination of surface vacancies and islands. Finally, the average effective interlayer current is seen to describe the conditions needed for favorable and smooth multilayer growth. These separate but closely interconnected problems have been approached by using different modeling and computational schemes.

Submonolayer growth has been studied using Rate Equation formulation. Rate equations provide a flexible and computationally effective tool to model complex island growth phenomena and are particularly suitable in IBAD and LEID type of growth conditions. In IBAD and LEID the surface is under constant ion bombardment and growth is thus explicitly a nonequilibrium phenomenon. The advantage of such HTD methods over the MBE is a higher deposition rate during the growth process. Also, control over the quality of the atomic layers is better. The main reasons for improvements are that the instabilities in island growth are suppressed due to ion bombardment. Second layer nucleation can start only at a very late stage of monolayer filling due to bombardment induced adatom detachment form large islands.

Description of the aggregation–detachment picture of submonolayer growth was ac-

complished in a simplified rate equation model. Island diffusion was taken into account using an approximation where the diffusion coefficient for islands follows a power law. Adatom detachment was described using the physical assumption that adatoms would detach with a probability per unit time that is directly proportional to the length of the island perimeter. This model is realistic for LEID and IBAD growth. The results showed an anomalously high adatom concentration compatible with LEID experiments. Also, a transition from fast growth (large growth exponent β) to slow growth (small growth exponent β) was observed within the experimentally accessible growth conditions, suggesting a growth parameter regime for optimum layer by layer growth (Paper I). The assumption of adatom detachment only from island edges was then tested in Molecular Dynamics simulations, and consequently shown to be reasonable (Paper II).

We further compared the LEID and IBAD methods from the point of view of ion bombardment induced break up, and the effect of it on the island size distributions. It was shown that in LEID adatom detachment is responsible for the enhanced adatom density on the surface. This is in contrast to IBAD where binary break-up of islands is a more favorable mode, and the island size distribution was narrower and distinctly peaked when compared to island size distribution in LEID. The effect of different break-up modes was also reflected in the growth exponents (Paper III).

In Paper IV we studied the effect of diffusion and surface geometry on island size distributions and growth exponents. Island diffusion on the fcc (1 0 0) and (1 1 1) surfaces differs drastically and may affect the growth. However, even though the growth exponents were observed to change due to the difference in diffusion they remained in the range of typical values for the models studied. Also, the scaled island density function was found to be of the typical form. This means that we were able to show that growth is robust with respect to the growth conditions, and the balance between the basic processes drives the growth.

The models used this far excluded the effect of surface vacancies on growth. In Paper V we studied the effect of interlayer recombination processes between islands and surface vacancies on growth. In the case where the substrate surface is allowed to develop single and island-like vacancies, more controlled growth and improved smoothness is possible, since vacancies may slow down growth by lowering the excess adatom density and preventing the coalescence of large islands in early stages of growth (in submonolayer regime). This in turn keeps the surface smoother until the late stages of growth when layer filling takes place and the second layer starts to nucleate.

Regarding multilayer growth a phenomenological model was studied in which the interlayer mass transfer was taken to depend solely on the difference in coverage on each layer. The model describes in a qualitative level the transition form the 3D growth mode and rough surfaces to the 2D layer-by-layer growth mode as encountered in LEID, and relates the change of the growth mode to the ion bombardment induced pile-up and insertion events of surface adatoms. It was found that the optimum window of bombarding energies predicted by the model for the layer-by-layer growth in LEID is from 5 eV to 25 eV, which is in agreement with MD and KMC simulation results reported previously in the corresponding cases (Paper VI).

The studies this far have been on a phenomenological level. There are several reasons for that. First, there is lack of experimental data on several key elements in the rate equation models. While island diffusion is theoretically quite well understood detailed measurements of the diffusion coefficient are few. There is still some controversy on mechanisms of island break-up, which are not completely understood based on the latest experiments. Our work suggests that there is possible improvement to be gained from experimental studies of island break-up. A more detailed knowledge of diffusion for islands on different surfaces and the detailed measurements of island break-up probabilities under various growth conditions could lead to more quantitative descriptions of growth in computationally inexpensive and flexible models,

which could be used to find the optimal growth conditions and extend the limits of the current thin film manufacturing methods. This ambitious goal remains beyond the scope of this Thesis and will be the object of future studies.

References

[1] C. A. Volkert and A. M. Minor. Focused ion beam microscopy and micromachining. *MRS Bulletin*, 32, May 2007.

[2] M. v. Smoluchowski. Drei Vortäge über Diffusion, Brownsche Molekularbewegung und Koagulation von Kolloidteilchen. *Physikalische Zeitschrift*, XVII: 585–598, September 1916. In German.

[3] M. v. Smoluchowski. Versuch einer matematischen Theorie der Koagulationskinetik kolloider Lösungen. *Zeitschrift für physikalische Chemie*, XCII:129–168, July 1917. In German.

[4] J. A. Venables, G. D. T. Spiller, and M. Hanbucken. Nucleation and growth of thin films. *Reports on Progress in Physics*, 47(4):399–459, 1984. URL `http://stacks.iop.org/0034-4885/47/399`.

[5] J. Feder, T. Jøssang, and E. Rosenqvist. Scaling behavior and cluster fractal dimension determined by light scattering from aggregating proteins. *Phys. Rev. Lett.*, 53(15):1403–1406, Oct 1984. doi: 10.1103/PhysRevLett.53.1403.

[6] S. Ispolatov, P. L. Krapivsky, and S. Redner. Wealth distributions in asset exchange models. *The European Physical Journal B*, 2:267–276, 1998.

[7] J. Silk and S. D. White. The development of structure in the expanding universe. *The Astrophysical Journal*, 223(2):L59, 1978.

[8] B. A. Joyce. Molecular beam epitaxy. *Rep. Prog. Phys.*, 1985.

[9] G B Stringfellow. Epitaxy. *Reports on Progress in Physics*, 45(5):469–525, 1982. URL `http://stacks.iop.org/0034-4885/45/469`.

[10] T. Suntola. Atomic layer epitaxy. *Materials Science Reports*, 4(7), 1989.

[11] B. Degroote, A. Vantomme, H. Pattyn, and K. Vanormelingen. Hyperthermal effects on nucleation and growth during low-energy ion deposition. *Phys. Rev. B*, 65:195401, April 2002.

[12] S. Esch, M. Breeman, M. Morgenstern, T. Michely, and G. Comsa. Nucleation and morphology of homoepitaxial Pt(111) -films grown with ion beam assisted deposition. *Surf. Sci.*, 365:187–204, 1996.

[13] S. Esch, M. Bott, T. Michely, and G. Comsa. Nucleation of homoepitaxial films grown with ion assistance on Pt(111). *Appl. Phys. Lett.*, 67(21):3209, November 1995.

[14] M. Kalff, M. Breeman, M. Morgenstern, T. Michely, and G. Comsa. Effect of energetic particles on island formation in sputter deposition of Pt on Pt(111). *Appl. Phys. Lett.*, 70(2):182, January 1997.

[15] J. M. Pomeroy, J. Jacobsen, B. H. Cooper, and J. P. Sethna. Kinetic Monte Carlo–molecular dynamics investigations of hyperthermal copper deposiotion on Cu(111). *Phys. Rev. B*, 66:235412, December 2002.

[16] T. Michely and G. Comsa. Generation and nucleation of adatoms during ion bombardment of Pt(111). *Phys. Rev. B*, 44(15):8411, October 1991.

[17] C.-H. Choi, R. Ai, and S. A. Barnett. Suppression of three-dimensional island nucleation during GaAs growth in Si(100). *Phys. Rev. Lett.*, 67(20):2826, November 1991.

[18] B. K. Kellerman, E. Chason, J. A. Floro, S. T. Picraux, and J. M. White. The role of transient ion-induced defects in ion beam-assisted growth. *Appl. Phys. Lett.*, 67(12):1703, September 1995.

[19] D. Adamovic, V. Chirita, E. P. Münger, L. Hultman, and J. E. Greene. Enhanced intra- and interlayer mass transport on Pt(111) via 5–50 eV Pt atom impacts on two-dimensional Pt clusters. *Thin Solid Films*, page 2235, 2006.

[20] J. Jacobsen, B. H. Cooper, and J. P. Sethna. Simulation of energetic beam deposition: From picoseconds to seconds. *Phys. Rev. B*, 58(23):15847, June 1998.

[21] A. Petersen, C. Busse, C. Polop, U. Linke, and T. Michely. From erosion to bombardment-induced growth on Ir(111). *Phys. Rev. B*, 68:245410, 2003.

[22] J. Sillanpää and I. T. Koponen. Island growth in ion beam assisted metal-on-metal deposition modelled by rate equations. *Nucl. Inst. Meth. B*, 142:67–76, 1998.

[23] R. J. Pflueger. Nucleation during epithermal bombardment of surfaces. *J. Chem. Phys.*, 105:1221–1236, 1996.

[24] Z. Q. Ma and Y. Kido. The atomic displacements on surface generated by low-energy projectile. *Thin Solid Films*, 359:288, 2000.

[25] B. Degroote. *Diffusion and Nucleation of Co on Ag(001), a Comparison of Thermal Deposition and Low Energy Ion Deposition.* PhD thesis, Katolieke Universiteit Leuven, 2001. Electronic address: http://fys.kuleuven.be/iks/nvsf/Files/thesis-bart.pdf.

[26] J. Heinonen, I. Koponen, J. Merikoski, and T. Ala-Nissilä. Island diffusion on metal fcc(100) surfaces. *Phys. Rev. Lett.*, 82(13):2733, March 1999.

[27] S. V. Khare and T. L. Einstein. Brownian motion and shape fluctuations of single-layer adatom and vacancy clusters on surfaces: Theory and simulations. *Phys. Rev. B*, 54(16):11752–11761, Oct 1996. doi: 10.1103/PhysRevB.54.11752.

[28] J. M. Soler. Cluster diffusion by evaporation-condensation. *Phys. Rev. B*, 53 (16):R10540–R10543, Apr 1996. doi: 10.1103/PhysRevB.53.R10540.

[29] M. Rusanen, I. T. Koponen, and J. Asikainen. Island growth in submonolayer deposition with aggregation and fragmentation. *Eur. Phys. J. B*, 36:567–572, September 2003.

[30] P. Hohenberg and W. Kohn. Inhomogeneous electron gas. *Phys. Rev.*, 136 (3B):B864–B871, Nov 1964. doi: 10.1103/PhysRev.136.B864.

[31] R. M. Martin. *Electronic structure : basic theory and practical methods.* Cambridge, UK ; New York : Cambridge University Press, 2004.

[32] A. Nagy. Density functional. theory and application to atoms and molecules. *Physics Reports*, 298(1):1–79, 1998.

[33] J. M. Haile. *Molecular dynamics simulation : elementary methods.* Wiley, New York, 1992.

[34] D. C. Rapaport. *The Art of Molecular Dynamics Simulation.* Cambridge University Press, Cambridge, England, 1995.

[35] D. P. Landau und K. Binder. *A Guide to Monte Carlo Simulations in Statistical Physics.* Cambridge University Press, Cambridge, 2000.

[36] J. W. Evans, P. A. Thiel, and M. C. Bartelt. Morpohological evolution during epitaxial thin film growth: Formation of 2d islands and 3d mounds. *Surf. Sci. Reports*, 61:1–128, 2006.

[37] P. G. J. van Dongen and M. H. Ernst. Dynamic scaling in the kinetics of clustering. *Phys. Rev. Lett.*, 54(13):1396, April 1985.

[38] F. Leyvraz. Scaling theory and exactly solved models in the kinetics of irreversible aggregation. *Physics Reports*, 383(2–3):95–212, August 2003.

[39] P. L. Krapivsky, J. F. F. Mendes, and S. Redner. Logarithmic islanding in submonolayer epitaxial growth. *Eur. Phys. J. B*, 4(4):401–404, July 1998.

[40] M. Rusanen. *Island Growth And Step Instabilities On Flat And Vicinal Surfaces.* PhD thesis, Laboratory of Physics Helsinki University of Technology, 2003.

[41] M. O. Jahma, M. Rusanen, A. Karim, I. T. Koponen, T. Ala-Nissila, and T. S. Rahman. Diffusion and submonolayer island growth during hyperthermal deposition on Cu(100) and Cu(111). *Surf. Sci.*, 598:246–252, 2005.

[42] K. Kyuno and G. Ehrlich. Cluster diffusion and dissociation in the kinetics of layer growth: An atomic view. *Phys. Rev. Lett.*, 84(12):2658, March 2000.

[43] W. Ensinger. Low energy ion assist during deposition — an effective tool for controlling thin film microstructure. *Nucl. Inst. Meth. B*, 127/128:796–808, 1997.

[44] I. T. Koponen, M. Rusanen, and J. Heinonen. Island size distributions in submonolayer growth with mobile islands and breakup. *Phys. Rev. E*, 58(3): 4037, September 1998.

[45] K. Kang and S. Redner. Fluctuation effects in Smoluchowski reaction kinetics. *Phys. Rev. A*, 30(5):2833, November 1984.

[46] K. Kang and S. Redner. Scaling approach for the kinetics of recombination processes. *Phys. Rev. Lett.*, 52(12):955, March 1984.

[47] K. Kang, S. Redner, P. Meakin, and F. Leyvraz. Long-time crossover phenomena in coagulation kinetics. *Phys. Rev. A*, 33(2):1171, February 1986.

[48] B. Degroote, A. Vantomme, K. Vanormelingen, and M. Hou. Low-energy ion deposition of Co on Ag(001): A molecular dynamics study. *Phys. Rev. B*, 65: 195402, April 2002.

[49] E. F. C. Haddeman B. S. Bunnik, C. de Hoog and B.J. Thijsse. Molecular dynamics study of Cu deposition on Mo and the effects of low-energy ion irradiation. *Nucl. Inst. Meth. B*, 187:57, 2002.

[50] G. Betz and W. Husinsky. A combined molecular dynamics and kinetic monte carlo calculation to study sputter erosion and beam assisted deposition. *Nucl. Inst. Meth. B*, 193:352, 2002.

[51] A. Bogicevic, S. Liu, J. Jacobsen, B. Lundqvist, and H. Metiu. Island migration caused by the motion of the atoms at the border: Size and temperature dependence of the diffusion coefficient. *Phys. Rev. B*, 57(16):R9459, April 1998.

[52] S. Pal and K. A. Fichthorn. Size dependence of the diffusion coefficient for large absorbed clusters. *Phys. Rev. B*, 60(11):7804, September 1999.

[53] S. C. Wang and G. Ehrlich. Structure, stability, and surface diffusion of clusters: Irx on Ir(111). *Surf. Sci.*, 239(3):301–332, December 1990.

[54] S. C. Wang and Gert Ehrlich. Diffusion of large surface clusters: Direct observations on Ir(111). *Phys. Rev. Lett.*, 79:4234–4237, 1997.

[55] S. C. Wang, U. Kürpick, and G. Ehrlich. Surface diffusion of compact and other clusters: Irx on Ir(111). *Phys. Rev. Lett.*, 81:4923–4926, 1998.

[56] J. M. Wen, S. L. Chang, J. W. Burnett, J. W. Evans, and P. A. Thiel. Diffusion of large two-dimensional Ag clusters on Ag(100). *Phys. Rev. Lett.*, 73:2591, 1994.

[57] K. Morgenstern, G. Rosenfeld, B. Poelsema, and G. Comsa. Brownian motion of vacancy islands on Ag(111). *Phys. Rev. Lett.*, 74:2058, 1995.

[58] K. Morgenstern, G. Rosenfeld, and G. Comsa. Decay of two-dimensional Ag islands on Ag(111). *Phys. Rev. Lett.*, 76:2113, 1996.

[59] W. W. Pai, A. K. Swan, Z. Zhang, and J. F. Wendelken. Island diffusion and coarsening on metal(100) surfaces. *Phys. Rev. Lett.*, 79(17):3210, October 1997.

[60] S. V. Khare, N. C. Bartelt, and T. L. Einstein. Diffusion of monolayer adatom and vacancy clusters: Langevin analysis and monte carlo simulation of their brownian motion. *Phys. Rev. Lett.*, 75(11):2148, September 1995.

[61] S. V. Khare and T. L. Einstein. Brownian motion and shape fluctuations of single-layer adatom and vacancy clusters on surfaces: Theory and simulations. *Phys. Rev. B*, 54:11752–11761, 1996.

[62] J. R. Sanchez and J. W. Evans. Diffusion of small clusters on metal(100) surfaces: Exact master-equation analysis for lattice-gas models. *Phys. Rev. B*, 59(4):3224, January 1999.

[63] O. S. Trushin, P. Salo, and T. Ala-Nissila. Energetics and many-particle mechanisms of two-dimensional cluster diffusion on Cu(100) surfaces. *Phys. Rev. B*, 62:1611, 2000.

[64] P. Salo, J. Hirvonen, I. T. Koponen, O. S. Trushin, J. Heinonen, and T. Ala-Nissilä. Role of concerted atomic movements in the diffusion of small islands on fcc(100) metal surfaces. *Phys. Rev. B*, 64:161405(R), October 2001. Rapid communcations.

[65] O. S. Trushin, P. Salo, M. Alatalo, and T. Ala-Nissila. Atomic mechanisms of cluster diffusion on metal fcc(100) surfaces. *Surf. Sci.*, 482–485:365–369, 2001.

[66] O. S. Trushin, J. Hirvonen, J. Heinonen, P. Salo, M. Alatalo, T. Ala-Nissila, I. T. Koponen, and J. Merikoski. Adatom island diffusion on metal fcc(100) surfaces. In M. C. Tringides and Z. Chvoj, editors, *Collective Diffusion on Surfaces: Correlation Effects and Adatom Interactions*, pages 317–325. Kluwer, 2001.

[67] G. S. Bales and A. Zangwill. Self-consistent rate theory of submonolayer homoeitaxy with attachment/detachment kinetics. *Phys. Rev. B*, 55(4):R1973, January 1997.

[68] C. Ratsch, A. Zangwill, P. Šmilauer, and D. D. Vvedensky. Saturation and scaling of epitaxial ispland densities. *Phys. Rev. Lett.*, 72(20):3194, May 1994.

[69] B. Degroote, J. Dekoster, and G. Langouche. Step decoration and surface

alloying: growth of cobalt on Ag(100) as a function of deposition temperature. *Surf. Sci.*, 452:172, 2000.

[70] W. A. Hofer, A. S. Foster, and A. L. Shluger. Theories of scanning probe microscopes at the atomic scale. *Rev. Mod. Phys.*, 75:1287, 2003.

[71] M. Weinelt, S. Shwarz, H. Baier, S. Müller, L. Hammer, K. Heinz, and Th. Fauster. Structure of ultrathin Fe films on Cu(100) prepared by pulsed laser deposition. *Phys. Rev. B*, 63:205413, 2001.

[72] F. Tsui, J. Wellman, C. Uher, and R. Clarke. Morphology transition and layer-by-layer growth of Rh(111). *Phys. Rev. Lett.*, 76:3164, 1996.

[73] R. Kunkel, B. Poelsema, L. K. Verheij, and G. Comsa. Reentrant layer-by-layer growth during molecular-beam epitaxy of metal-on-metal substrates. *Phys. Rev. Lett.*, 65:733, 1990.

[74] V. I. Trofimov, V. G. Mokerov, and A. G. Shumyankov. Kinetic model for molecular beam epitaxial growth on a singular surface. *Thin Solid Films*, 306: 105, 1997.

[75] I. T. Koponen. Modeling layer-by-layer growth in ion assisted deposition of thin films. *Nucl. Inst. Meth. B*, 171:314–324, 2000.

[76] J. Sillanpää, I. T. Koponen, and N. Grønbech-Jensen. A rate-equation model for the growth of metallic thin films in ion beam assisted deposition. *Nucl. Inst. Meth. B*, 184:523–530, 2001.

[77] M. G. Barthes and A. Rolland. The first stages in the formation of ultrathin nickel layers on Ag(111): A low energy electron diffraction-auger electron spectroscopy study. *Thin Solid Films*, 76:45, 1981.

[78] B. Voigtländer and T. Weber. Nucleation and growth of Si/Si(111) observed by scanning tunneling microscopy during epitaxy. *Phys. Rev. B*, 54:7709, 1996.

[79] Q. Fu and T. Wagner. Diffusion-corrected simultaneous multilayer growth model. *Phys. Rev. Lett.*, 90:106105, 2003.

[80] J. Krug, P. Politi, and T. Michely. Island nucleation in the presence of step-edge barriers: Theory and applications. *Phys. Rev. B*, 61:14037, 2000.

[81] K. J. Caspersen, C. R. Stoldt, A. K.Layson, M. C. Bartelt, P. A. Thiel, and J.W. Evans. Morphology of multilayer Ag/Ag(100) films versus deposition temperature: STM analysis and atomistic lattice-gas modeling. *Phys. Rev. B*, 63:085401, 2001.

[82] V.I. Trofimov and V.G. Mokerov. Rate equations model for layer epitaxial growth kinetics. *Thin Solid Films*, 428:66, 2003.

[83] V.I. Trofimov and V.G. Mokerov. Growth mode transitions and scaling behaviour at successive stages of molecular beam epitaxy. *Thin Solid Films*, 380: 67, 2000.

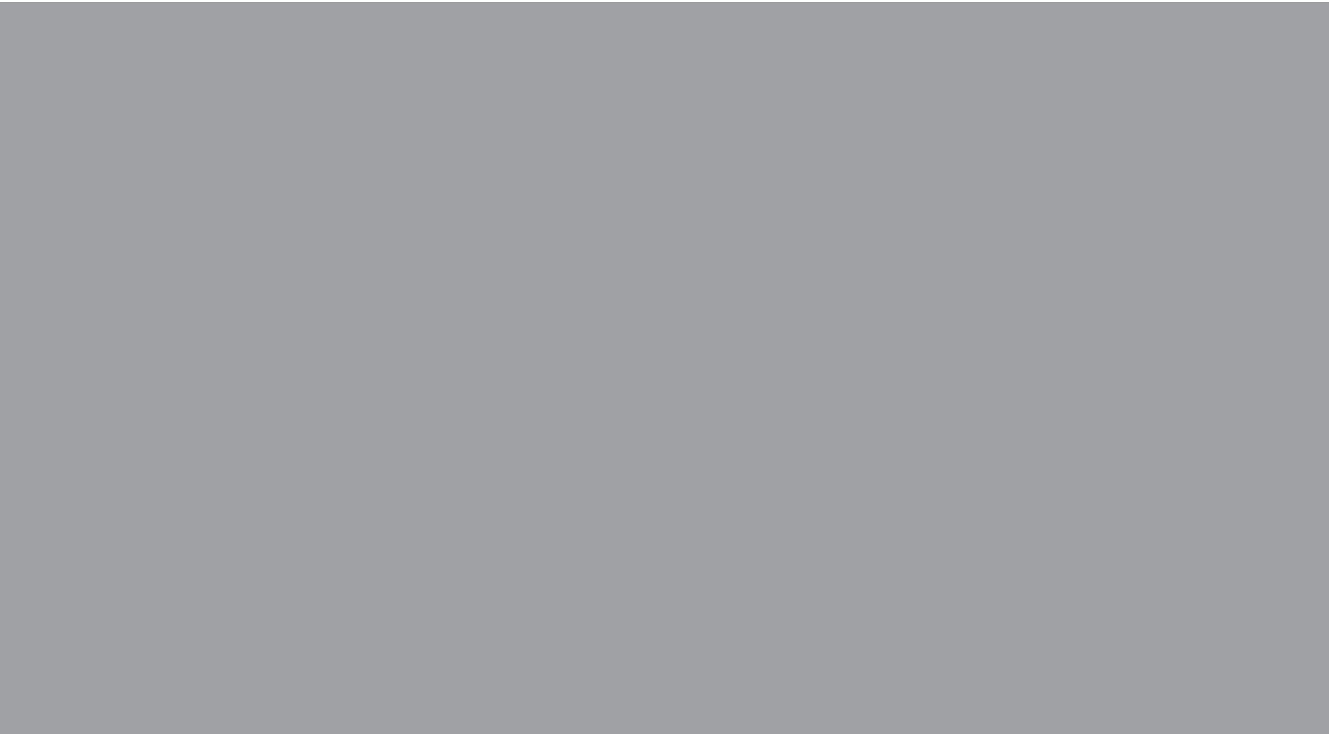

ISBN 978-951-22-9113-7
ISBN 978-951-22-9114-4 (PDF)
ISSN 1795-2239
ISSN 1795-4584 (PDF)